



Thermomechanical interactions in nonlocal thermoelastic medium with double porosity structure

Chandra Sekhar Mahato¹ · Siddhartha Biswas¹

Received: 17 November 2023 / Accepted: 31 January 2024
© The Author(s), under exclusive licence to Springer Nature B.V. 2024

Abstract

The main objective of this work is to create a new thermoelastic model for hyperbolic thermoelasticity in the context of double porosity structure based on nonlocal elasticity theory and the dual-phase-lag model. Nonlocal elasticity theory is used to construct new constitutive relations and equations. In a homogeneous, isotropic thermoelastic material, thermomechanical interactions are studied using normal mode analysis. A time-dependent thermal shock is applied on the boundary surface. This study also produces a few unique situations, which are compared with previous results of other researchers. The normal and tangential stresses, temperature, displacement components, change in void volume fractions, and equilibrated stress vectors concerning distances and time intervals are all calculated numerically. The physical quantities mentioned above are also visually displayed for various thermoelastic models to compare and illustrate the theoretical results. A comparative analysis and graphical presentation of the effects of nonlocal parameters and porosity on various physical characteristics have been performed. The figures show that most of the physical variables decrease with the increase in distance and show oscillatory behavior with the increase in time. The behavior of the void volume fraction field of the first kind is opposite to the behavior of the void volume fraction field of the second kind with the increase in distance. It is also noticed that the behavior of equilibrated stress of the first kind is opposite to the behavior of the second kind.

Keywords Thermomechanical interactions · Nonlocal · Double porosity · Dual-phase-lag model · Normal mode analysis

1 Introduction

The theory of elastic material with voids has been developed by Cowin and Nunziato (1983). According to this idea, the voids in the medium are considered empty pores with some surface area and volume but no mechanical or energetic significance. The bulk density of the material is expressed as a product of two fields: (i) the density of the matrix material and (ii) the void volume fractional field. This is the basic tenet of the linear theory of elastic material with voids. When an elastic solid with voids deforms, two fields are involved:

✉ S. Biswas
siddharthabsws957@gmail.com

¹ Department of Mathematics, University of North Bengal, Darjeeling, West Bengal, India

the strain field, which is related to the matrix material, and the change in the fractional field of void volume, which is related to the voids in the medium. Iesan and Quintanilla (2014) have developed a theory of thermoelastic solids with a double porosity structure based on the Nunziato and Cowin (1979) theory of elastic materials with voids. Puri and Cowin (1985) have derived the plane wave propagation in elastic material with voids and discovered three types of plane waves propagating at different speeds. Khalili and Selvaduri (2003) have proposed a comprehensive thermo-hydro-mechanical coupling model that takes several critical processes into account, and this model gives a holistic understanding of the thermo-hydro-mechanical behavior of materials, particularly for scenarios where temperature changes significantly affect the mechanical response and fluid flow within the system. Kumar et al. (2018) have investigated the propagation of Rayleigh waves in a homogeneous isotropic thermoelastic half-space with void characteristics, the surface of which is stress-free, thermally insulated, and isothermal. Iesan (1986) has proposed a linear theory of thermoelastic materials with void parameters. He investigated certain general theorems (uniqueness, reciprocal behavior, and variational), acceleration waves, and equilibrium difficulties in this theory. Abdou et al. (2020a) have investigated the effect of the magnetic field on a two-dimensional thermoelastic medium based on the Lord–Shulman theory of the body, which has a doubly porous structure. Singh et al. (2020) have developed a time-harmonic plane wave propagation within an infinite thermoelastic solid medium with a double porosity structure. Abdou et al. (2020b) have studied a general solution to the field equations of a generalized thermoelastic medium with double porosity under the Lord–Shulman model of thermoelasticity, the effect of the relaxation time on a two-dimensional thermoelastic medium that has a doubly porous structure in the presence of diffusion and gravity. Othman and Mansour (2023) studied the effect of relaxation time on a two-dimensional thermoelastic medium which has a doubly porous structure in the presence of diffusion and gravity.

Many authors have focused their attention on the nonlocal thermoelasticity hypothesis since it has played a vital role in resolving many previous issues in fracture mechanics. Nonlocal continuum field theories are concerned with the physics of material bodies whose behavior at a material point is influenced by the state of all points of the body. Following the classical notions, material points of a body are considered to be continuous and are assigned some physically independent objects (variables) (e.g., mass, charge, electric field, magnetic field). The state of the body, at a material point, is described by the relations of the response objects that constitute another class (e.g., stress, internal energy, heat) as functions of the independent objects. These relations are called constitutive equations. The nonlocal theory generalizes the classical field theory in two respects: (i) the energy balance law is considered valid globally (for the entire body), and (ii) the state of the body at a material point is described by the response functionals. In nonlocal elasticity, Eringen (1977) developed the problem of straight-edge dislocation. Eringen computed the stress retained and elastic energy in this case. Eringen (1974) used the theory of nonlocal thermoelasticity, which generated a set of constitutive equations for nonlocal thermoelastic substances. Eringen (1998) discovered a theory that combines electromagnetism with superconductivity. Eringen and Edelen (1972) also proposed a theory of nonlocal elasticity that includes two primary phases and gives an extensive framework for predicting the behavior of materials with nonlocal interactions at small scales. Kumar et al. (2021) investigated a linear theory of nonlocal elastic materials with a double porosity structure. The effect of a nonlocal model on a poro-thermoelastic solid with temperature-dependent properties with the help of a three-phase-lag model (3PHL) of thermoelasticity was studied by Othman et al. (2023).

In the literature on thermal effects, a classical Fourier law and generalized versions of Fourier law describe heat conduction. The classical thermoelasticity hypothesis, which is

based on the classical Fourier law of heat conduction, suffers from physically unrealistic phenomena because, in the parabolic-type heat conduction equation, the speed of the thermal signal is infinite. To remove this physically impossible occurrence, classical thermoelasticity models have been generalized. The heat flow in a hyperbolic-type problem is modeled with finite-speed thermal signals, and thermoelasticity theories admit such signals. Hyperbolic-type thermoelasticity (nonclassical thermoelasticity) theories eliminated unrealistic phenomena. Thermoelasticity with thermal relaxation is an extension of the classical theory of thermoelasticity that takes into account the time-dependent reaction of materials to temperature variations reviewed in Chandrasekharaiah (1998).

Lord and Shulman (1967) developed a generalized theory of thermoelasticity based on the Maxwell and the Cattaneo-Vernotte (CV) (generalized version of Fourier law) heat conduction equations. This modified thermoelasticity theory incorporated one relaxation time and altered the parabolic-type heat conduction equation into a hyperbolic-type equation, referred to as the LS model and widely employed in low-temperature and heat flux cases. Green and Lindsay (1972) derived a theory known as the GL theory, which involves two relaxation times.

The equation for Fourier's law of heat conduction is $q = -K \nabla T \dots (i)$. The Cattaneo-Vernotte (CV) equation, a modified form of Fourier's law, provides the base for the most fundamental linear hyperbolic heat conduction theory: $q + \tau \frac{\partial q}{\partial t} = -K \nabla T$. The next generalized thermoelasticity theory is the dual-phase-lag model (DPL) introduced by Tzou (1995). Tzou (1995) proposed the following generalization: $q(P, t + \tau_q) = -K \nabla T(P, t + \tau_T) \dots (ii)$. This relationship states that the heat flux vector at P at time $t + \tau_q$ corresponds to the temperature gradient at a point P of the material at time $t + \tau_T$. The delay time τ_T , also known as the phase lag of the temperature gradient, is understood to be the result of microstructural interactions, which are small-scale heat transport mechanisms that occur in microscale or small-scale effects of heat transport in space, such as photoelectron interaction or phonon scattering. The other delay time τ_q , also known as the phase lag of the heat flux, is understood as the relaxation time resulting from the fast-transient effects of thermal inertia (or small-scale impacts of heat transport in time). It is to be noted that the heat flux is the result (effect) of a temperature gradient in a transient process, the relation (ii) allows either the temperature gradient or the heat flux to become the effect and the remaining one the cause. A temperature gradient produces the heat flux vector for materials where $\tau_q > \tau_T$. The response between the temperature gradient and the heat flux is instantaneous if $\tau_q = \tau_T$ (which is not necessarily zero); in this scenario, the relation (ii) becomes the same as the classical Fourier law (i). Furthermore, it should be emphasised that although the connection (ii) is microscopic in both space and time, the conventional Fourier rule is macroscopic in both. Tzou (1995) describes the constitutive equation relating the heat flux vector and the temperature gradient as having a single-phase-lag model, denoted as $q(P, t + \tau_q) = -K \nabla T(P, t)$, and a dual-phase-lag model, denoted as relation (ii). According to his research (Tzou 1995), both of these models can be used within the context of the extended irreversible thermodynamics second law.

Green and Naghdi (1992, 1993) presented three models of generalized thermoelasticity of homogeneous isotropic materials, known as type I, II, and III models. The Green-Naghdi model is separated into two kinds based on the presence or absence of energy dissipation. The Green-Naghdi model of type II has thermoelasticity without energy dissipation. The Green-Naghdi model of type III couples thermoelasticity with energy dissipation. Said et al. (2022b) developed the three-phase-lag (TPL) model and the Green-Naghdi theory of types II and III with a memory-dependent derivative to study the effect of rotation on a nonlocal porous thermoelastic medium. In the context of the linearized theory of coupled thermoelasticity, Roy Choudhuri (2007) suggested a three-phase-lag model. This model takes into

account a heat conduction rule that includes the temperature gradient as well as the thermal displacement gradient as constitutive variables. This model is an extension of the Lord–Shulman, Green-Naghdi, and Tzou thermoelastic models. Sarkar et al. (2022) developed the Lord–Shulman theory for the propagation of the photo-thermal waves in a semiconducting nonlocal elastic medium.

Khurana and Tomar (2016) explored wave propagation in nonlocal micro-stretch solids. Kaur et al. (2021a) studied a novel model of forced vibrational analysis of nonlocal transversely isotropic thermoelastic nanobeam resonators due to ramp-type heating and time-varying exponentially decaying load with a multi-dual-phase-lag theory of thermoelasticity. Biswas and Mahato (2022) investigated Rayleigh waves in a nonlocal orthotropic layer resting over a nonlocal orthotropic half-space employing an eigenvalue technique in the context of a dual-phase-lag model. Kaur and Singh (2022a) studied vibrations in 2D functionally graded nanobeams (FGN) with memory-dependent derivatives. Gupta and Mukhopadhyay (2019) developed a study on the generalized thermoelasticity theory with the dual-phase-lag model based on a nonlocal heat conduction law. Khalili (2003) investigated the coupling effects in double porosity media with a deformable matrix. The eigenfunction expansion approach was presented by Biswas and Mukhopadhyay (2017) as an analytical technique for exploring thermal shock behavior in a magneto-thermoelastic orthotropic material. The research looks at how the three-phase-lag model affects the medium's response to thermal shock. Kaur and Singh (2023b) presented the coupled photo-thermoelastic analysis in semiconductor resonator with the nonlocal Memory dependent derivative (MDD) theory. Kalkal et al. (2021) studied a three-phase-lag functionally graded thermoelastic model with a twofold porosity structure and gravitational influence. Sherief and Saleh (2005) proposed the theory of generalized thermoelastic diffusion with a single relaxation time. This problem involves the coupling of thermal, elastic, and diffusive phenomena in a material with memory-dependent behavior. In the presence of void parameters, Biswas (2021) investigated the thermal shock behavior in a homogeneous orthotropic medium with the three-phase-lag model. Mondal et al. (2019) investigated waves in dual-phase-lag thermoelastic materials in the presence of void parameters based on Eringen's nonlocal elasticity theory. Kaur et al. (2023b) focused on recent research on thermoelasticity theories as well as their associated reformed models related to the micro-/nano-beams/nano-bars. A plane wave in nonlocal thermoelastic solid material with voids was discovered by Tomar and Sarkar (2019). The free energy and variational theorem of an elastic problem related to thermal shock were explored by Hong-Gang (1982). The impact of mechanical boundary conditions on the thermal shock resistance of ceramics used in ultra-high temperature applications was studied by Cheng et al. (2015). Said et al. (2021) used the theory of multi-phase-lags with fractional derivative heat transfer thermoelasticity to study the wave propagation on a nonlocal fiber-reinforced thermoelastic medium. Said et al. (2022a) analyzed the effect of gravity and initial stress on a nonlocal thermo-viscoelastic medium with two-temperature and fractional derivative heat transfer.

In this research, we investigate the constitutive relations and field equations of an isotropic thermoelastic material with double porosity structures. The theoretical structure used in Eringen's nonlocal theory of elasticity in spatial form enables us to account for nonlocal effects in the material responses. An extensive investigation has been done in the field of material science to investigate the thermal shock response in a nonlocal isotropic medium that is influenced by the existence of double porosity structures. The dual-phase-lag model of generalized thermoelasticity is employed to solve the problem. Normal mode analysis is employed to generate a differential equation, which is then solved. To the authors' knowledge, the effect of the dual-phase-lag model on thermoelastic material with

double porosity structure using nonlocal elasticity theory is not available in the literature to date. The comparison of different physical quantities for different models like dual-phase-lag (DPL), Lord–Shulman (LS), and classical coupled thermoelasticity (CT) are presented graphically in this paper, which was not found in any earlier published works. The values of physical variables, including displacements, stresses, void volume fraction field, temperature, and equilibrated stresses, are calculated numerically for different values of time and distance and presented graphically to compare and demonstrate the theoretical results. It is noticed that for different thermoelastic models, as well as in the presence and absence of nonlocal parameters and void parameters, different physical quantities such as displacement components, stresses, void volume fraction fields, temperature, and equilibrated stresses show oscillatory behavior with the increase in time. The equilibrated stress and void volume fraction field corresponding to the first kind of void show the opposite behavior to behavior of the equilibrated stress and void volume fraction field corresponding to the second kind of void. It is also observed that for different thermoelastic models, as well as in the presence and absence of nonlocal parameters, different physical quantities, such as displacement components and stresses, increase with increasing distance. The study of problems related to civil engineering takes advantage of the double porosity structure extensively. In mathematics and physics, the normal mode technique is a useful tool for finding the exact solution for specific physical structures, particularly those that exhibit harmonic activity. It is often used to analyze waves, vibrations, and oscillations in a variety of physical systems, including mechanical systems, electrical circuits, and quantum systems.

The structure of this work is as follows: Based on Eringen's nonlocal elasticity theory, we develop the relationship between double voids and nonlocal parameters in Sect. 2. We build the fundamental equations and constitutive relations in Sect. 2.1. We also derive the dual-phase-lag model within the context of nonlocal thermoelasticity. Section 2.1 also includes a nomenclature table. With the use of stress equations of motion (in the absence of body forces), equilibrated stress equations of motion (in the absence of extrinsic equilibrated body forces), and fundamental relations, we obtain the governing equations in Sect. 2.1. In Sect. 3, we develop the boundary conditions subjected to stress-free surface. In Sect. 4, we develop solution methodology via normal mode analysis and derive a 10th-order differential equation to find the eigenvalues. In Sect. 5, we find the solution using the regularity condition at $z \rightarrow \infty$ and also obtain the stress components. We deduce some limiting situations in Sect. 6. The comparison and validation of the work are covered in Sect. 7. The most important section, which includes a discussion of numerical and a graphical overview of the current work, is presented in Sect. 8. The impact of nonlocal parameters and double voids on various physical variables are visually displayed for several thermoelastic models in the numerical discussion section. Some important applications of the current work are provided in Sect. 9. The conclusion is given in Sect. 10.

2 Nonlocal formulation with double porosity

First, we establish the field equations and constitutive relations in a continuum thermoelastic body containing double porosity with the surface area S and volume V . Let $\mathbf{x} = (x_1, x_2, x_3)$ be any typical point of the considered body in the reference state and $\mathbf{x}' = (x'_1, x'_2, x'_3)$ be any surrounding point of \mathbf{x} .

Suppose $T = \theta - T_0$, where θ is the absolute temperature, T_0 is the initial temperature, and T is the temperature above reference temperature such that $|\frac{T}{T_0}| \ll 1$. We assume that

the set of basic variables at two neighboring point \mathbf{x} and \mathbf{x}' is given as follows:

$$\begin{aligned} X &= \{e_{ij}(\mathbf{x}), \phi(\mathbf{x}), \phi_{,i}(\mathbf{x}), \psi(\mathbf{x}), \psi_{,i}(\mathbf{x}), T(\mathbf{x})\}, \\ X' &= \{e_{ij}(\mathbf{x}'), \phi(\mathbf{x}'), \phi_{,i}(\mathbf{x}'), \psi(\mathbf{x}'), \psi_{,i}(\mathbf{x}'), T(\mathbf{x}')\}, \end{aligned} \tag{1}$$

where $e_{ij} = \frac{1}{2}(u_{i,j} + u_{j,i})$; ($i, j = 1, 2, 3$) are the Lagrangian strain tensor within the context of linear theory, u_i are the displacement vector during deformation process, $\phi = v_1(\mathbf{x}, t) - (v_1)_R$ and $\psi = v_2(\mathbf{x}, t) - (v_2)_R$ are the change in void volume fraction from the reference void volume corresponding to the first and second kind of voids, respectively. A comma (,) in the subscript denotes the spatial derivative.

The strain energy function W for nonlocal thermoelastic materials with double voids can be taken as (Eringen 1974; Biswas and Mahato 2022; Mahato and Biswas 2023):

$$\begin{aligned} 2W &= C_{ijkl}e_{ij}(\mathbf{x})e_{kl}(\mathbf{x}') + m\phi(\mathbf{x})\phi(\mathbf{x}') + p\psi(\mathbf{x})\psi(\mathbf{x}') + A_{ij}\phi_{,i}(\mathbf{x})\phi_{,i}(\mathbf{x}') + \gamma_{ij}\psi_{,i}(\mathbf{x})\psi_{,i}(\mathbf{x}') \\ &+ B_{ij}[e_{ij}(\mathbf{x})\phi(\mathbf{x}') + e_{ij}(\mathbf{x}')\phi(\mathbf{x})] + L_{ij}[e_{ij}(\mathbf{x})\psi(\mathbf{x}') + e_{ij}(\mathbf{x}')\psi(\mathbf{x})] \\ &+ D_{ijk}[e_{ij}(\mathbf{x})\phi_{,k}(\mathbf{x}') + e_{ij}(\mathbf{x}')\phi_{,k}(\mathbf{x})] + E_{ijk}[e_{ij}(\mathbf{x})\psi_{,k}(\mathbf{x}') + e_{ij}(\mathbf{x}')\psi_{,k}(\mathbf{x})] \\ &+ D_i[\phi(\mathbf{x})\phi_{,i}(\mathbf{x}') + \phi(\mathbf{x}')\phi_{,i}(\mathbf{x})] + E_i[\psi(\mathbf{x})\psi_{,i}(\mathbf{x}') + \psi(\mathbf{x}')\psi_{,i}(\mathbf{x})] \\ &+ b_{ij}[\phi_{,i}(\mathbf{x})\psi_{,j}(\mathbf{x}') + \phi_{,i}(\mathbf{x}')\psi_{,j}(\mathbf{x})] + \alpha_1[\phi(\mathbf{x})\psi(\mathbf{x}') + \phi(\mathbf{x}')\psi(\mathbf{x})] \\ &+ b_i[\phi(\mathbf{x})\psi_{,i}(\mathbf{x}') + \phi(\mathbf{x}')\psi_{,i}(\mathbf{x})] + d_i[\phi_{,i}(\mathbf{x})\psi(\mathbf{x}') + \phi_{,i}(\mathbf{x}')\psi(\mathbf{x})] \\ &- \beta_{ij}[e_{ij}(\mathbf{x})T(\mathbf{x}') + e_{ij}(\mathbf{x}')T(\mathbf{x})] - aT(\mathbf{x})T(\mathbf{x}') - \gamma_1[\phi(\mathbf{x})T(\mathbf{x}') + \phi(\mathbf{x}')T(\mathbf{x})] \\ &- \gamma_2[\psi(\mathbf{x})T(\mathbf{x}') + \psi(\mathbf{x}')T(\mathbf{x})] - a_i[\phi_{,i}(\mathbf{x})T(\mathbf{x}') + \phi_{,i}(\mathbf{x}')T(\mathbf{x})] \\ &- h_i[\psi_{,i}(\mathbf{x})T(\mathbf{x}') + \psi_{,i}(\mathbf{x}')T(\mathbf{x})], \end{aligned} \tag{2}$$

where C_{ijkl} , m , p , A_{ij} , γ_{ij} , B_{ij} , L_{ij} , D_{ijk} , E_{ijk} , D_i , E_i , b_{ij} , α_1 , b_i , d_i , a , γ_1 , γ_2 , a_i and h_i are the constitutive coefficients and prescribed function of the positions \mathbf{x} and \mathbf{x}' .

Following Eringen (1974, 1977) and Mahato and Biswas (2023) the constitutive relations can be obtained from the relation:

$$\Gamma = \int_V \left[\frac{\partial W}{\partial X} + \left(\frac{\partial W}{\partial X'} \right)^s \right] dV(\mathbf{x}'), \tag{3}$$

where the superscript 's' represents the symmetry of that quantity with respect to the interchange of \mathbf{x} and \mathbf{x}' .

Further, the set $\Gamma = \{\tau_{ij}, \sigma_i, -\xi, \tau_i, -\zeta, -\rho\eta\}$ is an ordered set with the set X .

Using (1) and (3), we obtain the following:

$$\tau_{ij} = \int_V \left[\frac{\partial W}{\partial e_{ij}(\mathbf{x})} + \left(\frac{\partial W}{\partial e_{ij}(\mathbf{x}')} \right)^s \right] dV(\mathbf{x}'), \tag{4}$$

$$\sigma_i = \int_V \left[\frac{\partial W}{\partial \phi_{,i}(\mathbf{x})} + \left(\frac{\partial W}{\partial \phi_{,i}(\mathbf{x}')} \right)^s \right] dV(\mathbf{x}'), \tag{5}$$

$$-\xi = \int_V \left[\frac{\partial W}{\partial \phi(\mathbf{x})} + \left(\frac{\partial W}{\partial \phi(\mathbf{x}')} \right)^s \right] dV(\mathbf{x}'), \tag{6}$$

$$\tau_i = \int_V \left[\frac{\partial W}{\partial \psi_{,i}(\mathbf{x})} + \left(\frac{\partial W}{\partial \psi_{,i}(\mathbf{x}')} \right)^s \right] dV(\mathbf{x}'), \tag{7}$$

$$-\zeta = \int_V \left[\frac{\partial W}{\partial \psi(\mathbf{x})} + \left(\frac{\partial W}{\partial \psi(\mathbf{x}')} \right)^s \right] dV(\mathbf{x}'), \tag{8}$$

$$\rho\eta = \int_V \left[\frac{\partial W}{\partial T(\mathbf{x})} + \left(\frac{\partial W}{\partial T(\mathbf{x}')} \right)^s \right] dV(\mathbf{x}'). \tag{9}$$

Inserting (2) into (4)-(9), we obtain

$$\begin{aligned} \tau_{ij} = \int_V [& C_{ijkl}(\mathbf{x}, \mathbf{x}')e_{kl}(\mathbf{x}') + B_{ij}(\mathbf{x}, \mathbf{x}')\phi(\mathbf{x}') + L_{ij}(\mathbf{x}, \mathbf{x}')\psi(\mathbf{x}') \\ & + D_{ijk}(\mathbf{x}, \mathbf{x}')\phi_{,k}(\mathbf{x}') + E_{ijk}(\mathbf{x}, \mathbf{x}')\psi_{,k}(\mathbf{x}') - \beta_{ij}(\mathbf{x}, \mathbf{x}')T(\mathbf{x}')] dV(\mathbf{x}'), \end{aligned} \tag{10}$$

$$\begin{aligned} \sigma_i = \int_V [& D_{kli}(\mathbf{x}, \mathbf{x}')e_{kl}(\mathbf{x}') + A_{ij}(\mathbf{x}, \mathbf{x}')\phi_{,j}(\mathbf{x}') + b_{ij}(\mathbf{x}, \mathbf{x}')\psi_{,j}(\mathbf{x}') \\ & + D_i(\mathbf{x}, \mathbf{x}')\phi(\mathbf{x}') + d_i(\mathbf{x}, \mathbf{x}')\psi(\mathbf{x}')] dV(\mathbf{x}'), \end{aligned} \tag{11}$$

$$\begin{aligned} \xi = - \int_V [& m(\mathbf{x}, \mathbf{x}')\phi(\mathbf{x}') + B_{ij}(\mathbf{x}, \mathbf{x}')e_{ij}(\mathbf{x}') + D_i(\mathbf{x}, \mathbf{x}')\phi_{,i}(\mathbf{x}') + \alpha_1(\mathbf{x}, \mathbf{x}')\psi(\mathbf{x}') \\ & + b_i(\mathbf{x}, \mathbf{x}')\psi_{,i}(\mathbf{x}') - \gamma_1(\mathbf{x}, \mathbf{x}')T(\mathbf{x}')] dV(\mathbf{x}'), \end{aligned} \tag{12}$$

$$\begin{aligned} \tau_i = \int_V [& E_{kli}(\mathbf{x}, \mathbf{x}')e_{kl}(\mathbf{x}') + \gamma_{ij}(\mathbf{x}, \mathbf{x}')\psi_{,j}(\mathbf{x}') + b_{ij}(\mathbf{x}, \mathbf{x}')\phi_{,j}(\mathbf{x}') + E_i(\mathbf{x}, \mathbf{x}')\psi(\mathbf{x}') \\ & + b_i(\mathbf{x}, \mathbf{x}')\phi(\mathbf{x}')] dV(\mathbf{x}'), \end{aligned} \tag{13}$$

$$\begin{aligned} \zeta = - \int_V [& l(\mathbf{x}, \mathbf{x}')\phi(\mathbf{x}') + L_{ij}(\mathbf{x}, \mathbf{x}')e_{ij}(\mathbf{x}') + E_i(\mathbf{x}, \mathbf{x}')\psi_{,i}(\mathbf{x}') + p(\mathbf{x}, \mathbf{x}')\psi(\mathbf{x}') \\ & + d_i(\mathbf{x}, \mathbf{x}')\phi_{,i}(\mathbf{x}') - \gamma_2(\mathbf{x}, \mathbf{x}')T(\mathbf{x}')] dV(\mathbf{x}'), \end{aligned} \tag{14}$$

$$\begin{aligned} \rho\eta = \int_V [& \beta_{ij}(\mathbf{x}, \mathbf{x}')e_{ij}(\mathbf{x}') + a(\mathbf{x}, \mathbf{x}')T(\mathbf{x}') + \gamma_1(\mathbf{x}, \mathbf{x}')\phi(\mathbf{x}') + \gamma_2(\mathbf{x}, \mathbf{x}')\psi(\mathbf{x}') \\ & + a_i(\mathbf{x}, \mathbf{x}')\phi_{,i}(\mathbf{x}') + h_i(\mathbf{x}, \mathbf{x}')\psi_{,i}(\mathbf{x}')] dV(\mathbf{x}'), \end{aligned} \tag{15}$$

For centrosymmetric, isotropic material, the constitutive coefficients are given by

$$\begin{aligned} D_{ijk} &= E_{ijk} = D_i = E_i = d_i = b_i = a_i = h_i = 0, \\ C_{ijkl}(\mathbf{x}, \mathbf{x}') &= \lambda(\mathbf{x}, \mathbf{x}')\delta_{ij}\delta_{kl} + 2\mu(\mathbf{x}, \mathbf{x}')\delta_{ik}\delta_{jl}, \\ (A_{ij}, B_{ij}, b_{ij}, \gamma_{ij}, L_{ij}, \beta_{ij})(\mathbf{x}, \mathbf{x}') &= (\alpha, h, b_1, \gamma, d, \beta)(\mathbf{x}, \mathbf{x}')\delta_{ij}, \end{aligned}$$

where the quantities $\alpha, h, b_1, \gamma, d, \gamma_1, \gamma_2$ and a are constitutive coefficients. All the constitutive coefficients are functions of $|\mathbf{x} - \mathbf{x}'|$ and attenuate with distance because, for most of the materials, the cohesive zone is very small. Furthermore, within the cohesive zone, the intermolecular forces decrease rapidly with distance from the reference point, i.e.,

$$\lim_{(|\mathbf{x} - \mathbf{x}'| \rightarrow \infty)} \lambda(|\mathbf{x} - \mathbf{x}'|) \rightarrow 0,$$

etc.

Thus, constitutive relations (10)-(15) become

$$\begin{aligned} \tau_{ij} = & \int_V [\lambda(|\mathbf{x} - \mathbf{x}'|)\delta_{ij}e_{kk}(\mathbf{x}') + 2\mu(|\mathbf{x} - \mathbf{x}'|)e_{ij}(\mathbf{x}') + h(|\mathbf{x} - \mathbf{x}'|)\delta_{ij}\phi(\mathbf{x}') \\ & + d(|\mathbf{x} - \mathbf{x}'|)\delta_{ij}\psi(\mathbf{x}') - \beta(|\mathbf{x} - \mathbf{x}'|)\delta_{ij}T(\mathbf{x}')]dV(\mathbf{x}'), \end{aligned} \quad (16)$$

$$\sigma_i = \int_V [\alpha(|\mathbf{x} - \mathbf{x}'|)\phi_{,i}(\mathbf{x}') + b_1(|\mathbf{x} - \mathbf{x}'|)\psi_{,i}(\mathbf{x}')]dV(\mathbf{x}'), \quad (17)$$

$$\begin{aligned} \xi = & - \int_V [m(|\mathbf{x} - \mathbf{x}'|)\phi(\mathbf{x}') + h(|\mathbf{x} - \mathbf{x}'|)e_{ii}(\mathbf{x}') + \alpha_1(|\mathbf{x} - \mathbf{x}'|)\psi(\mathbf{x}') \\ & - \gamma_1(|\mathbf{x} - \mathbf{x}'|)T(\mathbf{x}')]dV(\mathbf{x}'), \end{aligned} \quad (18)$$

$$\tau_i = \int_V [b_1(|\mathbf{x} - \mathbf{x}'|)\phi_{,i}(\mathbf{x}') + \gamma(|\mathbf{x} - \mathbf{x}'|)\psi_{,i}(\mathbf{x}')]dV(\mathbf{x}'), \quad (19)$$

$$\begin{aligned} \zeta = & - \int_V [l(|\mathbf{x} - \mathbf{x}'|)\phi(\mathbf{x}') + d(|\mathbf{x} - \mathbf{x}'|)e_{ii}(\mathbf{x}') + p(|\mathbf{x} - \mathbf{x}'|)\psi(\mathbf{x}') \\ & - \gamma_2(|\mathbf{x} - \mathbf{x}'|)T(\mathbf{x}')]dV(\mathbf{x}'), \end{aligned} \quad (20)$$

$$\begin{aligned} \rho\eta = & \int_V [\beta(|\mathbf{x} - \mathbf{x}'|)e_{ii}(\mathbf{x}') + a(|\mathbf{x} - \mathbf{x}'|)T(\mathbf{x}') + \gamma_1(|\mathbf{x} - \mathbf{x}'|)\phi(\mathbf{x}') \\ & + \gamma_2(|\mathbf{x} - \mathbf{x}'|)\psi(\mathbf{x}')]dV(\mathbf{x}'). \end{aligned} \quad (21)$$

The constitutive coefficients are assumed to attenuate to the same degree and reach their peaks at $\mathbf{x} = \mathbf{x}'$. Therefore, we can take the following relation between nonlocal coefficients (with unprimed notations) and local elastic coefficients (with primed notations) as:

$$\begin{aligned} (\lambda, \mu, h, d, \alpha, \gamma, m, p, \alpha_1, b_1, a, \gamma_1, \gamma_2)(\mathbf{x}, \mathbf{x}') = & (\lambda', \mu', h', d', \alpha', \gamma', m', p', \alpha'_1, b'_1, \\ & a', \gamma'_1, \gamma'_2,)G(|\mathbf{x} - \mathbf{x}'|, \chi), \end{aligned} \quad (22)$$

where $G(|\mathbf{x} - \mathbf{x}'|, \chi)$ is a nonlocal kernel expressing the effect of remote point \mathbf{x}' to the point \mathbf{x} . Here, $\chi = \frac{\varepsilon}{l}$, where ε ($= e_0 a_{cl}$) is the nonlocal parameter, e_0 is the material constant, l is the external characteristic length, and a_{cl} is the internal characteristic length of the material.

$G(|\mathbf{x} - \mathbf{x}'|, \chi)$ has the following properties:

- (i) $\int_V G(|\mathbf{x} - \mathbf{x}'|, \chi)dV(\mathbf{x}') = 1$.
- (ii) The function G attains its peak at $(|\mathbf{x} - \mathbf{x}'| = 0)$ and generally decays with increasing $(|\mathbf{x} - \mathbf{x}'|)$.
- (iii) Following Eringen (1974, 1977), we have

$$(1 - \varepsilon^2 \nabla^2)G(|\mathbf{x} - \mathbf{x}'|, \chi) = \delta(|\mathbf{x} - \mathbf{x}'|), \quad (23)$$

where $\nabla^2 = \frac{\partial^2}{\partial x^2} + \frac{\partial^2}{\partial y^2} + \frac{\partial^2}{\partial z^2}$.

2.1 Basic equations and constitutive relations

Operating $(1 - \varepsilon^2 \nabla^2)$ on the equations (16)-(21) and employing (22) and (23), we get the constitutive relations for a uniform nonlocal isotropic thermoelastic material possessing double porosity structure as follows:

$$(1 - \varepsilon^2 \nabla^2) \tau_{ij} = \tau_{ij}^L = \lambda' \delta_{ij} e_{kk}(\mathbf{x}) + 2\mu' e_{ij}(\mathbf{x}) + h' \delta_{ij} \phi(\mathbf{x}) + d' \delta_{ij} \psi(\mathbf{x}) - \beta' \delta_{ij} T(\mathbf{x}), \tag{24}$$

$$(1 - \varepsilon^2 \nabla^2) \sigma_i = \sigma_i^L = \alpha' \phi_{,i}(\mathbf{x}) + b'_1 \psi_{,i}(\mathbf{x}), \tag{25}$$

$$(1 - \varepsilon^2 \nabla^2) \xi = \xi^L = -m' \phi(\mathbf{x}) - h' e_{ii}(\mathbf{x}) - \alpha'_1 \psi(x) + \gamma'_1 T(\mathbf{x}), \tag{26}$$

$$(1 - \varepsilon^2 \nabla^2) \tau_i = \tau_i^L = b'_1 \phi_{,i}(\mathbf{x}) + \gamma' \psi_{,i}(\mathbf{x}), \tag{27}$$

$$(1 - \varepsilon^2 \nabla^2) \zeta = \zeta^L = -\alpha'_1 \phi(\mathbf{x}) - d' e_{ii}(\mathbf{x}) - p' \psi(x) + \gamma'_2 T(\mathbf{x}), \tag{28}$$

$$(1 - \varepsilon^2 \nabla^2) \rho \eta = (\rho \eta)^L = \beta' e_{ii}(\mathbf{x}) + \gamma'_1 \phi(\mathbf{x}) + \gamma'_2 \psi(\mathbf{x}) + a' T(\mathbf{x}). \tag{29}$$

Where the Dirac delta function has the following property:

$$\int f(x) \delta(x - a) dx = f(a).$$

We propose an Eringen-type Fourier law for the nonlocal generalization of the dual-phase-lag model as

$$(1 - \varepsilon^2 \nabla^2) \left(1 + \tau_q \frac{\partial}{\partial t} \right) q_i = \left(1 + \tau_q \frac{\partial}{\partial t} \right) q_i^L = -K \left(1 + \tau_T \frac{\partial}{\partial t} \right) T_{,i}(\mathbf{x}), \tag{30}$$

$$(1 - \varepsilon^2 \nabla^2) \rho \eta = (\rho \eta)^L = \beta' e_{ii}(\mathbf{x}) + \gamma'_1 \phi(\mathbf{x}) + \gamma'_2 \psi(\mathbf{x}) + a' T(\mathbf{x}). \tag{31}$$

The energy equation is

$$q_{i,i} = -\rho T_0 \dot{\eta}. \tag{32}$$

Operating $(1 - \varepsilon^2 \nabla^2)$ on the equation (32) and using (30) and (31), we get

$$\begin{aligned} & K \left(1 + \tau_T \frac{\partial}{\partial t} \right) T_{,ii}(\mathbf{x}) \\ &= \left(1 + \tau_q \frac{\partial}{\partial t} \right) (\beta' T_0 \dot{e}_{ii}(\mathbf{x}) + \gamma'_1 T_0 \dot{\phi}(\mathbf{x}) + \gamma'_2 T_0 \dot{\psi}(\mathbf{x}) + \rho C_v \dot{T}(\mathbf{x})), \end{aligned} \tag{33}$$

where $aT_0 = \rho C_v$.

Following Iesan and Quintanilla (2014), we have stress equations of motion:

$$\tau_{ij,j}^L = \rho \ddot{u}_i, \tag{34}$$

and equilibrated stress equations of motion:

$$\sigma_{i,i}^L + \xi^L = \chi_1 \ddot{\phi}, \tag{35}$$

$$\tau_{i,i}^L + \zeta^L = \chi_2 \ddot{\psi}. \tag{36}$$

Table 1 Nomenclature

Symbols	Descriptions	Symbols	Descriptions
τ_{ij}	Nonlocal components of the stress tensor	τ_q, τ_T	Phase-lags corresponding to heat flux vector and temperature gradient, respectively
τ_{ij}^L	Local components of the stress tensor	q_i	Nonlocal components of heat flux vectors
λ, μ	Lame's constants	C_v	Specific heat at constant strain
h, d	The coupling of void volume fractions of each type of voids with the normal stress	e_{ij}^L	Local components of strain tensors
α, γ	Couple the gradient of void volume fractions	K	Thermal conductivity
$\beta, \gamma_1, \gamma_2$	Thermal parameters	δ_{ij}	Kronecker delta
v_1, v_2	Void volume fractions	ρ	Mass density
ϕ, ψ	Change in void volume fraction from the reference void volume fraction	T_0	Reference temperature
η	Specific entropy per unit volume	α_t	Coefficients of linear thermal expansion
σ_i, τ_i	Nonlocal equilibrated stresses vectors	ξ, ζ	Nonlocal intrinsic equilibrated body force densities
b_1	Acts as a cross-coupling between the gradient of both void volume fractions and equilibrated stresses	α_1	Acts as a cross-coupling between void volume fractions and the intrinsic equilibrated body force densities
γ_1, γ_2	The thermo-void coefficients of first and second kinds of voids, respectively	q_i^L	Local components of the heat flux vector
σ_i^L, τ_i^L	Local equilibrated stress vectors	m, p	Void parameters
χ_1, χ_2	The equilibrated inertia per unit mass per unit volume corresponding to the first and second kinds of voids	u, w	Displacement components
ξ^L, ζ^L	Local intrinsic equilibrated body force densities	e_{ij}	Nonlocal components of strain tensors

Using Eqns. (24)–(28) in equations (34)–(36) and omitting prime ($'$) from the constitutive coefficients, the governing equations for a homogeneous isotropic nonlocal thermoelastic material with a double porosity structure can be written as follows:

$$(\lambda + 2\mu)u_{,xx} + \mu u_{,zz} + (\lambda + \mu)w_{,xz} + h\phi_{,x} + d\psi_{,x} - \beta T_{,x} = (1 - \varepsilon^2 \nabla^2)\rho \ddot{u}, \quad (37)$$

$$(\lambda + \mu)u_{,xz} + \mu w_{,xx} + (\lambda + 2\mu)w_{,zz} + h\phi_{,z} + d\psi_{,z} - \beta T_{,z} = (1 - \varepsilon^2 \nabla^2)\rho \ddot{w}, \quad (38)$$

$$\alpha(\phi_{,xx} + \phi_{,zz}) + b_1(\psi_{,xx} + \psi_{,zz}) - h(u_{,x} + w_{,z}) - m\phi - \alpha_1\psi + \gamma_1 T = (1 - \varepsilon^2 \nabla^2)\chi_1 \ddot{\phi}, \quad (39)$$

$$b_1(\phi_{,xx} + \phi_{,zz}) + \gamma(\psi_{,xx} + \psi_{,zz}) - d(u_{,x} + w_{,z}) - \alpha_1\phi - p\psi + \gamma_2 T = (1 - \varepsilon^2 \nabla^2)\chi_2 \ddot{\psi}, \quad (40)$$

$$K \left(1 + \tau_T \frac{\partial}{\partial t} \right) \nabla^2 T = \left(1 + \tau_q \frac{\partial}{\partial t} \right) (\beta T_0 \dot{e} + \gamma_1 T_0 \dot{\phi} + \gamma_2 T_0 \dot{\psi} + \rho C_v \dot{T}). \quad (41)$$

The physical significance of various coefficients is given as follows:

The coupling between the normal stress and the void volume fractions of each type of void is represented by the coefficients h and d . The gradient of the void volume fractions ϕ and ψ is coupled by the parameters α and γ to the associated equilibrated stress vectors σ_i and τ_i , which correspond to the first and second kinds of voids, respectively. The gradients of the equilibrated stresses and the void volume fractions are cross-coupled by the parameters b_1 . Furthermore, the parameter l acts as a cross-coupling between void volume fractions and the intrinsic equilibrated body force densities; γ_1 and γ_2 are the thermo-void coefficients of the first and second kinds of voids, respectively. The parameters m and p couple the void volume fractions ϕ and ψ with the intrinsic equilibrated body force densities ξ and ζ , respectively (Table 1).

3 Boundary conditions

We examine the scenario in which there is no traction on the surface and a time-dependent thermal shock applied to the half-space. To find the parameters A_n ($n = 1, 2, 3, 4, 5$), we consider the following boundary conditions at $z = 0$:

- (a) Thermal boundary condition that the surface of the half-space is subjected to a time-dependent thermal shock:

$$T(x, 0, t) = F(t)H(\vartheta - |x|), \tag{42}$$

where H is the Heaviside function.

- (b) Mechanical boundary condition that the surface to the half-space is traction free:

- (i)

$$\begin{aligned} \tau_{zz}(x, 0, t) &= 0 \\ \Rightarrow (1 - \varepsilon^2 \nabla^2) \tau_{zz}(x, 0, t) &= 0 \end{aligned}$$

which gives

$$\tau_{zz}^L(x, 0, t) = 0. \tag{43}$$

- (ii)

$$\begin{aligned} \tau_{xz}(x, 0, t) &= 0 \\ \Rightarrow (1 - \varepsilon^2 \nabla^2) \tau_{xz}(x, 0, t) &= 0 \end{aligned}$$

which gives

$$\tau_{xz}^L(x, 0, t) = 0. \tag{44}$$

- (c) Conditions on equilibrated stress components:

- (i)

$$\begin{aligned} \sigma_z(x, 0, t) &= 0 \\ \Rightarrow (1 - \varepsilon^2 \nabla^2) \sigma_z(x, 0, t) &= 0 \end{aligned}$$

which gives

$$\sigma_z^L(x, 0, t) = 0. \tag{45}$$

(ii)

$$\begin{aligned}\tau_z(x, 0, t) &= 0 \\ \Rightarrow (1 - \varepsilon^2 \nabla^2) \tau_z(x, 0, t) &= 0\end{aligned}$$

which gives

$$\tau_z^L(x, 0, t) = 0. \quad (46)$$

4 Solution methodology

The normal mode technique is an effective tool for determining the precise solution for particular physical structures, especially those that show harmonic activity, in the field of mathematics and physics. It is widely used in the study of oscillations, vibrations, and waves in a range of physical systems, such as quantum, mechanical, and electrical circuits. The physical variables that are significant as a superposition of normal modes are included in the normal mode technique. To solve equations (37)-(41), we employ normal mode analysis and consider the solution as given below:

$$(u, w, \phi, \psi, T)(x, z, t) = (\bar{u}, \bar{w}, \bar{\phi}, \bar{\psi}, \bar{T})(z) \exp[ik(x - ct)], \quad (47)$$

where \bar{u} , \bar{w} , $\bar{\phi}$, $\bar{\psi}$ and \bar{T} are the amplitudes of the physical quantities, k is the wave number, c is the phase velocity in the direction of x -axis. With the help of equation (47), equations (37)-(41), we reduce to the following forms:

$$(D^2 + a_1)\bar{u} + a_2 D\bar{w} + a_3 \bar{\phi} + a_4 \bar{\psi} + a_5 \bar{T} = 0, \quad (48)$$

$$a_7 D\bar{u} + (D^2 + a_6)\bar{w} + a_8 D\bar{\phi} + a_9 D\bar{\psi} + a_{10} D\bar{T} = 0, \quad (49)$$

$$a_{15}\bar{u} + a_{12} D\bar{w} + (D^2 + a_{11})\bar{\phi} + (a_{13} D^2 + a_{14})\bar{\psi} + a_{16} \bar{T} = 0, \quad (50)$$

$$a_{19}\bar{u} + a_{20} D\bar{w} + (a_{17} D^2 + a_{18})\bar{\phi} + (D^2 + a_{21})\bar{\psi} + a_{22} \bar{T} = 0, \quad (51)$$

$$a_{24}\bar{u} + a_{23} D\bar{w} + a_{26} \bar{\phi} + a_{27} \bar{\psi} + (D^2 + a_{25})\bar{T} = 0, \quad (52)$$

where

$$a_1 = \frac{\rho k^2 c^2 (1 + \varepsilon^2 k^2) - k^2 (\lambda + 2\mu)}{\mu - \rho \varepsilon^2 k^2 c^2}, a_2 = \frac{ik(\lambda + \mu)}{\mu - \rho \varepsilon^2 k^2 c^2}, a_3 = \frac{ikh}{\mu - \rho \varepsilon^2 k^2 c^2},$$

$$a_4 = \frac{ikd}{\mu - \rho \varepsilon^2 k^2 c^2}, a_5 = \frac{-ik\beta}{\mu - \rho \varepsilon^2 k^2 c^2}, a_6 = \frac{\rho k^2 c^2 (1 + \varepsilon^2 k^2) - \mu k^2}{\lambda + 2\mu - \rho \varepsilon^2 k^2 c^2},$$

$$a_7 = \frac{ik(\lambda + \mu)}{\lambda + 2\mu - \rho \varepsilon^2 k^2 c^2}, a_8 = \frac{h}{\lambda + 2\mu - \rho \varepsilon^2 k^2 c^2}, a_9 = \frac{d}{\lambda + 2\mu - \rho \varepsilon^2 k^2 c^2},$$

$$a_{10} = \frac{-\beta}{\lambda + 2\mu - \rho \varepsilon^2 k^2 c^2}, a_{11} = \frac{\chi_1 k^2 c^2 (1 + \varepsilon^2 k^2) - \alpha k^2 - m}{\alpha - \chi_1 \varepsilon^2 k^2 c^2},$$

$$a_{12} = \frac{-h}{\alpha - \chi_1 \varepsilon^2 k^2 c^2}, a_{13} = \frac{b_1}{\alpha - \chi_1 \varepsilon^2 k^2 c^2}, a_{14} = \frac{-(b_1 k^2 + \alpha_1)}{\alpha - \chi_1 \varepsilon^2 k^2 c^2}, a_{15} = \frac{-ikh}{\alpha - \chi_1 \varepsilon^2 k^2 c^2},$$

$$\begin{aligned}
 a_{16} &= \frac{\gamma_1}{\alpha - \chi_1 \varepsilon^2 k^2 c^2}, a_{17} = \frac{b_1}{\gamma - \chi_2 \varepsilon^2 k^2 c^2}, a_{18} = \frac{-(b_1 k^2 + \alpha_1)}{\gamma - \chi_2 \varepsilon^2 k^2 c^2}, a_{19} = \frac{-ikd}{\gamma - \chi_2 \varepsilon^2 k^2 c^2}, \\
 a_{20} &= \frac{-d}{\gamma - \chi_2 \varepsilon^2 k^2 c^2}, a_{21} = \frac{\chi_2 k^2 c^2 (1 + \varepsilon^2 k^2) - \alpha k^2 - m}{\gamma - \chi_2 \varepsilon^2 k^2 c^2}, a_{22} = \frac{\gamma_2}{\gamma - \chi_2 \varepsilon^2 k^2 c^2}, \\
 a_{23} &= \frac{ikcT_0\beta\tau_1}{K\tau_2}, a_{24} = \frac{-k^2cT_0\beta\tau_1}{K\tau_2}, a_{25} = \frac{ikc\rho C_v\tau_1}{K\tau_2} - k^2, \\
 a_{26} &= \frac{ikcT_0\gamma_1\tau_1}{K\tau_2}, a_{27} = \frac{ikcT_0\gamma_2\tau_1}{K\tau_2}.
 \end{aligned}$$

The condition for the existence of a nontrivial solution of the system of homogeneous equations (48)-(52) provide the following tenth-order differential equation:

$$[D^{10} + N_1 D^8 + N_2 D^6 + N_3 D^4 + N_4 D^2 + N_5](\bar{u}, \bar{w}, \bar{\phi}, \bar{\psi}, \bar{T})(z) = 0, \tag{53}$$

where $D \equiv \frac{d}{dz}$ and $N_n (n = 1, 2, 3, 4, 5)$ are provided in Appendix A.

5 Solution of the differential equation

Assuming the regularity condition at infinity, the solution of Eqn. (53) is obtained as

$$(\bar{u}, \bar{w}, \bar{\phi}, \bar{\psi}, \bar{T})(z) = \sum_{n=1}^5 (A_n, B_n, C_n, D_n, E_n) \exp[-\lambda_n z]. \tag{54}$$

Inserting Eqn. (54) into the Eqns. (48)-(52), we obtain the following relations:

$$B_n = x_n A_n, C_n = y_n A_n, D_n = z_n A_n, E_n = e_n A_n$$

From Eqn. (47), the displacement components, void volume fractions, and temperature are obtained as:

$$u = \sum_{n=1}^5 A_n \exp[-\lambda_n z + ik(x - ct)], \tag{55}$$

$$w = \sum_{n=1}^5 B_n \exp[-\lambda_n z + ik(x - ct)], \tag{56}$$

$$\phi = \sum_{n=1}^5 C_n \exp[-\lambda_n z + ik(x - ct)], \tag{57}$$

$$\psi = \sum_{n=1}^5 D_n \exp[-\lambda_n z + ik(x - ct)], \tag{58}$$

$$T = \sum_{n=1}^5 E_n \exp[-\lambda_n z + ik(x - ct)]. \tag{59}$$

The stress components are obtained as:

$$\begin{aligned} (1 - \varepsilon^2 \nabla^2) \tau_{xx} &= \tau_{xx}^L = (\lambda + 2\mu) \frac{\partial u}{\partial x} + \lambda \frac{\partial w}{\partial z} + h\phi + d\psi - \beta T \\ &= \sum_{n=1}^5 [ik(\lambda + 2\mu) - \lambda\lambda_n x_n + hy_n + dz_n - \beta e_n] A_n \exp[-\lambda_n z + ik(x - ct)], \end{aligned} \quad (60)$$

$$\begin{aligned} (1 - \varepsilon^2 \nabla^2) \tau_{zz} &= \tau_{zz}^L = (\lambda + 2\mu) \frac{\partial w}{\partial z} + \lambda \frac{\partial u}{\partial x} + h\phi + d\psi - \beta T \\ &= \sum_{n=1}^5 [ik\lambda - (\lambda + 2\mu)\lambda_n x_n + hy_n + dz_n - \beta e_n] A_n \exp[-\lambda_n z + ik(x - ct)], \end{aligned} \quad (61)$$

$$(1 - \varepsilon^2 \nabla^2) \tau_{xz} = \tau_{xz}^L = \mu \left(\frac{\partial u}{\partial z} + \frac{\partial w}{\partial x} \right) = \sum_{n=1}^5 [\mu (ikx_n - \lambda_n)] A_n \exp[-\lambda_n z + ik(x - ct)], \quad (62)$$

where

$$\begin{aligned} x_n &= \frac{-F_n}{G_n}, \quad y_n = \frac{x_n(P_n R_n - k_n U_n) + (P_n Q_n - J_n U_n)}{L_n U_n - P_n T_n}, \quad z_n = \frac{-(J_n + x_n k_n + y_n L_n)}{P_n}, \\ F_n &= \lambda_n [a_{10}(\lambda_n^2 + a_1) - a_5 a_7], \quad G_n = (a_5 - a_2 a_{10}) \lambda_n^2 + a_5 a_6, \quad J_n = a_{16}(\lambda_n^2 + a_1) - a_5 a_{15}, \\ K_n &= (a_5 a_{12} - a_2 a_{16}) \lambda_n, \quad L_n = a_3 a_{16} - a_5 (\lambda_n^2 + a_{11}), \quad P_n = a_4 a_{16} - a_5 (a_{13} \lambda_n^2 + a_{14}), \\ Q_n &= a_{22}(\lambda_n^2 + a_1) - a_5 a_{19}, \quad R_n = (a_5 a_{20} - a_2 a_{22}) \lambda_n, \quad T_n = a_3 a_{22} - a_5 (a_{17} \lambda_n^2 + a_{18}), \\ U_n &= a_4 a_{22} - a_5 (\lambda_n^2 + a_{21}) \quad (n = 1, 2, 3, 4, 5). \end{aligned}$$

Substituting from the expressions of considered variables into the above boundary conditions (42)-(46), we can obtain the following equations:

$$e_1 A_1 + e_2 A_2 + e_3 A_3 + e_4 A_4 + e_5 A_5 = G, \quad (63)$$

$$g_1 A_1 + g_2 A_2 + g_3 A_3 + g_4 A_4 + g_5 A_5 = 0, \quad (64)$$

$$f_1 A_1 + f_2 A_2 + f_3 A_3 + f_4 A_4 + f_5 A_5 = 0, \quad (65)$$

$$l_1 A_1 + l_2 A_2 + l_3 A_3 + l_4 A_4 + l_5 A_5 = 0, \quad (66)$$

$$m_1 A_1 + m_2 A_2 + m_3 A_3 + m_4 A_4 + m_5 A_5 = 0, \quad (67)$$

where

$$G = F(t)H(\vartheta - |x|) \exp[-ik(x - ct)], \quad e_n = \frac{a_{23} x_n \lambda_n - a_{24} - a_{26} y_n - a_{27} z_n}{\lambda_n^2 + a_{25}},$$

$$g_n = ik\lambda - \lambda_n x_n (\lambda + 2\mu) + hy_n + dz_n - \beta e_n, \quad f_n = \mu (ikx_n - \lambda_n), \quad l_n = \lambda_n (\alpha y_n + b_1 z_n),$$

$$m_n = \lambda_n (b_1 y_n + \gamma z_n); \quad (n = 1, 2, 3, 4, 5)$$

Eqns. (63)-(67) can be solved by Cramer’s rule for the unknowns A_1, A_2, A_3, A_4, A_5 . Solving, we obtain $A_1 = \frac{\Delta_1}{\Delta}, A_2 = \frac{\Delta_2}{\Delta}, A_3 = \frac{\Delta_3}{\Delta}, A_4 = \frac{\Delta_4}{\Delta}, A_5 = \frac{\Delta_5}{\Delta}$ where $\Delta, \Delta_n(n = 1, 2, 3, 4, 5)$ are given in the Appendix B.

6 Limiting cases

By considering different particular values of the parameters, we can derive some results as follows:

(a) Lord–Shulman (LS) model:

If we take $\tau_q = \tau$ and $\tau_T = 0$, then the present study reduces to the case of Lord–Shulman (LS) model. Now Eqns. (37)-(41) take the following form:

$$\begin{aligned}
 &(\lambda + 2\mu)u_{,xx} + \mu u_{,zz} + (\lambda + \mu)w_{,xz} + h\phi_{,x} + d\psi_{,x} - \beta T_{,x} = (1 - \varepsilon^2 \nabla^2)\rho \ddot{u}, \\
 &(\lambda + \mu)u_{,xz} + \mu w_{,xx} + (\lambda + 2\mu)w_{,zz} + h\phi_{,z} + d\psi_{,z} - \beta T_{,z} = (1 - \varepsilon^2 \nabla^2)\rho \ddot{w}, \\
 &\alpha(\phi_{,xx} + \phi_{,zz}) + b_1(\psi_{,xx} + \psi_{,zz}) - h(u_{,x} + w_{,z}) - m\phi - \alpha_1\psi + \gamma_1 T = (1 - \varepsilon^2 \nabla^2)\chi_1 \ddot{\phi}, \\
 &b_1(\phi_{,xx} + \phi_{,zz}) + \gamma(\psi_{,xx} + \psi_{,zz}) - d(u_{,x} + w_{,z}) - \alpha_1\phi - p\psi + \gamma_2 T = (1 - \varepsilon^2 \nabla^2)\chi_2 \ddot{\psi}, \\
 &K \nabla^2 T = \left(1 + \tau \frac{\partial}{\partial t}\right) (\beta T_0 \dot{e} + \gamma_1 T_0 \dot{\phi} + \gamma_2 T_0 \dot{\psi} + \rho C_v \dot{T}).
 \end{aligned}$$

(b) Coupled thermoelasticity (CT):

The current analysis reduces to the scenario of the conventional coupled thermoelasticity (CT) theory if we assume that $\tau_q = \tau_T = 0$. The fundamental equations in this case reduce to the following form:

$$\begin{aligned}
 &(\lambda + 2\mu)u_{,xx} + \mu u_{,zz} + (\lambda + \mu)w_{,xz} + h\phi_{,x} + d\psi_{,x} - \beta T_{,x} = (1 - \varepsilon^2 \nabla^2)\rho \ddot{u}, \\
 &(\lambda + \mu)u_{,xz} + \mu w_{,xx} + (\lambda + 2\mu)w_{,zz} + h\phi_{,z} + d\psi_{,z} - \beta T_{,z} = (1 - \varepsilon^2 \nabla^2)\rho \ddot{w}, \\
 &\alpha(\phi_{,xx} + \phi_{,zz}) + b_1(\psi_{,xx} + \psi_{,zz}) - h(u_{,x} + w_{,z}) - m\phi - \alpha_1\psi + \gamma_1 T = (1 - \varepsilon^2 \nabla^2)\chi_1 \ddot{\phi}, \\
 &b_1(\phi_{,xx} + \phi_{,zz}) + \gamma(\psi_{,xx} + \psi_{,zz}) - d(u_{,x} + w_{,z}) - \alpha_1\phi - p\psi + \gamma_2 T = (1 - \varepsilon^2 \nabla^2)\chi_2 \ddot{\psi}, \\
 &K \nabla^2 T = \beta T_0 \dot{e} + \gamma_1 T_0 \dot{\phi} + \gamma_2 T_0 \dot{\psi} + \rho C_v \dot{T}.
 \end{aligned}$$

7 Comparison and validation of the work

In this section, we discuss some special and particular cases by considering different particular values of the parameters and comparing them with the existing literature as follows:

(a) Nonlocal elastic medium with double porosity:

When the thermal coefficient is absent, that is, when $\beta = \gamma_1 = \gamma_2 = K = 0$. The present problem can be reduced to nonlocal elastic materials that have two voids. The current result then agrees with Kumar et al. (2021). Thus, we have the following fundamental equations:

$$\begin{aligned}(\lambda + 2\mu)u_{,xx} + \mu u_{,zz} + (\lambda + \mu)w_{,xz} + h\phi_{,x} + d\psi_{,x} &= (1 - \varepsilon^2 \nabla^2)\rho\ddot{u}, \\(\lambda + \mu)u_{,xz} + \mu w_{,xx} + (\lambda + 2\mu)w_{,zz} + h\phi_{,z} + d\psi_{,z} &= (1 - \varepsilon^2 \nabla^2)\rho\ddot{w}, \\ \alpha(\phi_{,xx} + \phi_{,zz}) + b_1(\psi_{,xx} + \psi_{,zz}) - h(u_{,x} + w_{,z}) - m\phi - \alpha_1\psi &= (1 - \varepsilon^2 \nabla^2)\chi_1\ddot{\phi}, \\ b_1(\phi_{,xx} + \phi_{,zz}) + \gamma(\psi_{,xx} + \psi_{,zz}) - d(u_{,x} + w_{,z}) - \alpha_1 l\phi - p\psi &= (1 - \varepsilon^2 \nabla^2)\chi_2\ddot{\psi}.\end{aligned}$$

(b) Local thermoelastic medium with double porosity:

If we take $\varepsilon = 0$, then the present study reduces to the local thermoelastic materials with double porosity, and the present result agrees with Iesan and Quintanilla (2014). In this case, the basic equations reduce to the following form:

$$\begin{aligned}(\lambda + 2\mu)u_{,xx} + \mu u_{,zz} + (\lambda + \mu)w_{,xz} + h\phi_{,x} + d\psi_{,x} - \beta T_{,x} &= \rho\ddot{u}, \\(\lambda + \mu)u_{,xz} + \mu w_{,xx} + (\lambda + 2\mu)w_{,zz} + h\phi_{,z} + d\psi_{,z} - \beta T_{,z} &= \rho\ddot{w}, \\ \alpha(\phi_{,xx} + \phi_{,zz}) + b_1(\psi_{,xx} + \psi_{,zz}) - h(u_{,x} + w_{,z}) - m\phi - \alpha_1\psi + \gamma_1 T &= \chi_1\ddot{\phi}, \\ b_1(\phi_{,xx} + \phi_{,zz}) + \gamma(\psi_{,xx} + \psi_{,zz}) - d(u_{,x} + w_{,z}) - \alpha_1\phi - p\psi + \gamma_2 T &= \chi_2\ddot{\psi}, \\ K\left(1 + \tau_T \frac{\partial}{\partial t}\right)\nabla^2 T &= \left(1 + \tau_q \frac{\partial}{\partial t}\right)(\beta T_0 \dot{e} + \gamma_1 T_0 \dot{\phi} + \gamma_2 T_0 \dot{\psi} + \rho C_v \dot{T}).\end{aligned}$$

(c) Nonlocal thermoelastic medium without double porosity:

The present study reduces to a nonlocal thermoelastic medium without voids by neglecting the constitutive constants corresponding to the first and second kinds of voids by setting the quantities $h, d, \alpha, b_1, \gamma, \gamma_1, \gamma_2, l, m, p, \chi_1, \chi_2$ to zero, which agrees with Gupta and Mukhopadhyay (2019). The fundamental equations now assume the form:

$$\begin{aligned}(\lambda + 2\mu)u_{,xx} + \mu u_{,zz} + (\lambda + \mu)w_{,xz} - \beta T_{,x} &= (1 - \varepsilon^2 \nabla^2)\rho\ddot{u}, \\(\lambda + \mu)u_{,xz} + \mu w_{,xx} + (\lambda + 2\mu)w_{,zz} - \beta T_{,z} &= (1 - \varepsilon^2 \nabla^2)\rho\ddot{w}, \\ K\left(1 + \tau_T \frac{\partial}{\partial t}\right)\nabla^2 T &= \left(1 + \tau_q \frac{\partial}{\partial t}\right)(\beta T_0 \dot{e} + \rho C_v \dot{T}).\end{aligned}$$

(d) Local thermoelastic medium without porosity:

If we take $\varepsilon = 0$ and neglect the constitutive constants corresponding to first and second kinds of voids by setting the quantities $h, d, \alpha, b_1, \gamma, \gamma_1, \gamma_2, l, m, p, \chi_1, \chi_2$ to zero, the present study reduces to nonlocal thermoelastic materials without voids and agrees with Biswas and Mukhopadhyay (2017) (replacing the three-phase-lag model by the dual-phase-lag model and taking isotropic materials instead of orthotropic materials) with suitable modifications. We derive the fundamental equations as follows:

$$(\lambda + 2\mu)u_{,xx} + \mu u_{,zz} + (\lambda + \mu)w_{,xz} - \beta T_{,x} = \rho\ddot{u},$$

$$(\lambda + \mu)u_{,xz} + \mu w_{,xx} + (\lambda + 2\mu)w_{,zz} - \beta T_{,z} = \rho \ddot{w},$$

$$K \left(1 + \tau_T \frac{\partial}{\partial t} \right) \nabla^2 T = \left(1 + \tau_q \frac{\partial}{\partial t} \right) (\beta T_0 \dot{e} + \rho C_v \dot{T}).$$

(e) Local thermoelastic medium with single porosity:

If we set $\varepsilon = 0$ and neglect the constitutive constants corresponding to second kind of voids by setting the quantities $d, b_1, \gamma, \gamma_2, l, p, \chi_2$ to zero, the present study reduces to the local thermoelastic materials with single voids and agrees with Biswas (2021) (replacing three-phase-lag model by dual-phase-lag model and taking isotropic materials instead of orthotropic materials) and Iesan (1986). The basic equations now become:

$$(\lambda + 2\mu)u_{,xx} + \mu u_{,zz} + (\lambda + \mu)w_{,xz} + h\phi_{,x} - \beta T_{,x} = \rho \ddot{u},$$

$$(\lambda + \mu)u_{,xz} + \mu w_{,xx} + (\lambda + 2\mu)w_{,zz} + h\phi_{,z} - \beta T_{,z} = \rho \ddot{w},$$

$$\alpha(\phi_{,xx} + \phi_{,zz}) - h(u_{,x} + w_{,z}) - m\phi + \gamma_1 T = \chi_1 \ddot{\phi},$$

$$K \left(1 + \tau_T \frac{\partial}{\partial t} \right) \nabla^2 T = \left(1 + \tau_q \frac{\partial}{\partial t} \right) (\beta T_0 \dot{e} + \gamma_1 T_0 \dot{\phi} + \rho C_v \dot{T}).$$

(f) Nonlocal thermoelastic medium with single porosity:

The present investigation reduces to nonlocal thermoelastic materials with single voids, which agrees with Mondal et al. (2019), if we set the constitutive constants $d, b_1, \gamma, \gamma_2, l, p, \chi_2$ to zero. In addition to the aforementioned requirement, the current conclusion coincides with Tomar and Sarkar (2019) if we assume $\tau_q = \tau$ and $\tau_T = 0$. The basic equations are reduced to

$$(\lambda + 2\mu)u_{,xx} + \mu u_{,zz} + (\lambda + \mu)w_{,xz} + h\phi_{,x} - \beta T_{,x} = (1 - \varepsilon^2 \nabla^2) \rho \ddot{u},$$

$$(\lambda + \mu)u_{,xz} + \mu w_{,xx} + (\lambda + 2\mu)w_{,zz} + h\phi_{,z} - \beta T_{,z} = (1 - \varepsilon^2 \nabla^2) \rho \ddot{w},$$

$$\alpha(\phi_{,xx} + \phi_{,zz}) - h(u_{,x} + w_{,z}) - m\phi + \gamma_1 T = (1 - \varepsilon^2 \nabla^2) \chi_1 \ddot{\phi},$$

$$K \left(1 + \tau_T \frac{\partial}{\partial t} \right) \nabla^2 T = \left(1 + \tau_q \frac{\partial}{\partial t} \right) (\beta T_0 \dot{e} + \gamma_1 T_0 \dot{\phi} + \rho C_v \dot{T}).$$

8 Numerical results and discussion

We know that the thermal shock is time dependent, so we consider $F(t) = \theta_0 \exp(-bt)$, where θ_0 is constant. For numerical computations, we consider the data values of copper material, which is given in Table 2

Table 2 Numerical values of various constants

Symbols	Values	Symbols	Values	Supporting refs.
λ	$7.76 \times 10^{10} \text{ Nm}^{-2}$	μ	$3.86 \times 10^{10} \text{ Nm}^{-2}$	Sherief and Saleh (2005), Mahato and Biswas (2023)
C_v	$3.831 \times 10^3 \text{ m}^2 \text{ s}^{-2} \text{ K}^{-1}$	K	$3.86 \times 10^3 \text{ N s}^{-1} \text{ K}^{-1}$	
ρ	$8.954 \times 10^3 \text{ kg m}^{-3} \text{ s}$	T_0	293 K	
α_t	$1.78 \times 10^{-5} \text{ K}^{-1}$	ε	0.009 m	
h	$0.9 \times 10^{10} \text{ Nm}^{-2}$	d	$0.1 \times 10^{10} \text{ Nm}^{-2}$	
b_1	$0.12 \times 10^{-5} \text{ N}$	γ	$1.1 \times 10^{-5} \text{ N}$	
γ_1	$0.16 \times 10^5 \text{ Nm}^{-2}$	γ_2	$0.219 \times 10^5 \text{ Nm}^{-2}$	
p	$2.4 \times 10^{10} \text{ Nm}^{-2}$	l	$2.5 \times 10^{10} \text{ Nm}^{-2}$	
m	$2.3 \times 10^{10} \text{ Nm}^{-2}$	χ_1	$0.1456 \times 10^{-12} \text{ Nm}^{-2} \text{ s}^2$	
χ_2	$0.1546 \times 10^{-12} \text{ Nm}^{-2} \text{ s}^2$	θ_0	100	
b	0.1 m	k	1.2 m^{-1}	
τ_q	0.05 s	τ_T	0.015 s	
x	0 m	ϑ	1	

8.1 Effect of different thermoelastic models on different physical quantities with respect to time

Figure 1 shows the variation of horizontal displacement component u with respect to time t for three different models of thermoelasticity, including DPL (Dual-phase-lag), LS (Lord–Shulman), and CT (coupled thermoelasticity) models. As time t increases, it is found that the horizontal displacement component u exhibits wave-type propagation. In the range of $3.34 \text{ s} < t < 7 \text{ s}$, the value of the horizontal displacement component u for the LS model is located between the values for the CT and DPL models. For the CT model, the value of u is at maximum.

Figure 2 depicts the comparison of T with different values of t for different thermoelastic models DPL, LS, and CT. For these three models, the value of w decreases as time t increases. For the CT model, T is at its highest value, and for the DPL model, it is at its smallest value. The value of T for the LS model lies between the value of w for CT and the DPL model.

Figure 3 illustrates the variations of tangential stress component τ_{xz} with the various values of t for different thermoelastic models. It is noticed that tangential stress component τ_{xz} is showing wave-type nature with the increase in time t . The tangential stress component τ_{xz} for the DPL model has a value that falls between the value for the CT and LS models with respect to tangential stress. The value of tangential stress component τ_{xz} attains its maximum for CT models and minimum for LS models.

Figure 4 shows a comparison of void volume fraction fields ψ with respect to different values of t in the presence of different thermoelastic models DPL, LS, and CT. In Fig. 4, ψ shows wave-type propagation with the increase in t . In particular, for the regions $1 \text{ s} < t < 2.01 \text{ s}$, $3.21 \text{ s} < t < 4.52 \text{ s}$, and $5.61 \text{ s} < t < 6.85 \text{ s}$, the value of the void volume fraction fields ψ for the CT model is less than for the LS model. The value of void volume fraction fields ψ for the CT model is higher than for the LS model for the regions $2.01 \text{ s} < t < 3.21 \text{ s}$ and $4.52 \text{ s} < t < 5.61 \text{ s}$. It can be analyzed from Figs. 3 and 4 that ϕ has reverse behavior to that of ψ .

Figure 5 represents the variation of equilibrated stress component σ_z with the different values of t . Wave-type nature can be observed from Fig. 5 of equilibrated stress component

Fig. 1 Comparison of horizontal displacement component u with respect to time (t) for different thermoelastic models

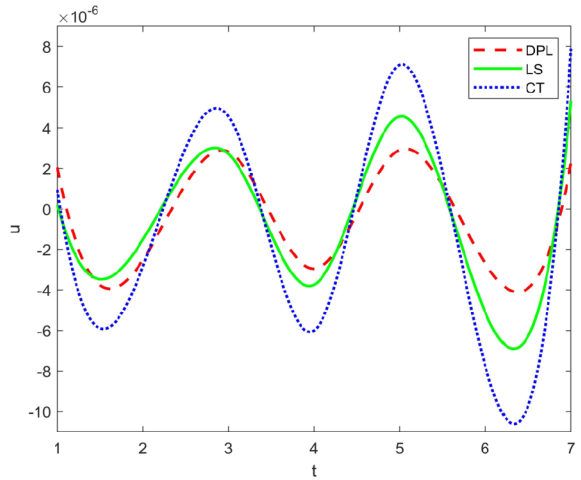


Fig. 2 Comparison of T with respect to time (t) for different thermoelastic models

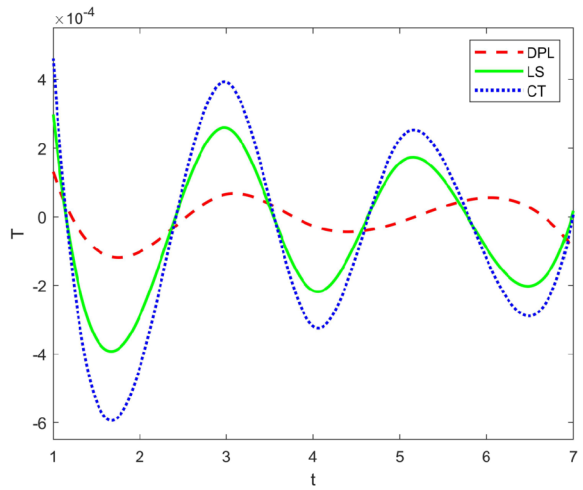


Fig. 3 Comparison of tangential stress component (τ_{xz}) with respect to time (t) for different thermoelastic models

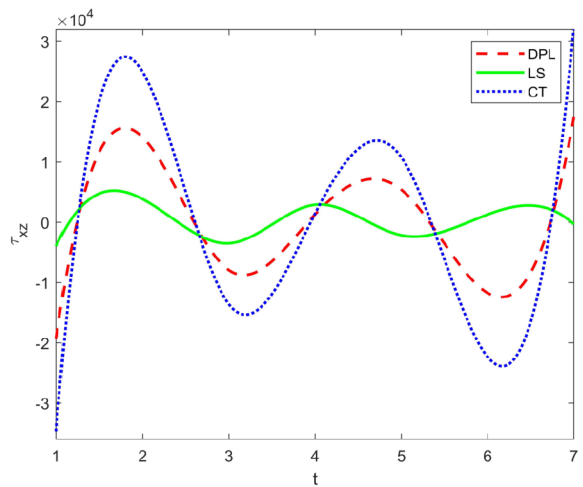


Fig. 4 Comparison of ψ with respect to time (t) for different thermoelastic models

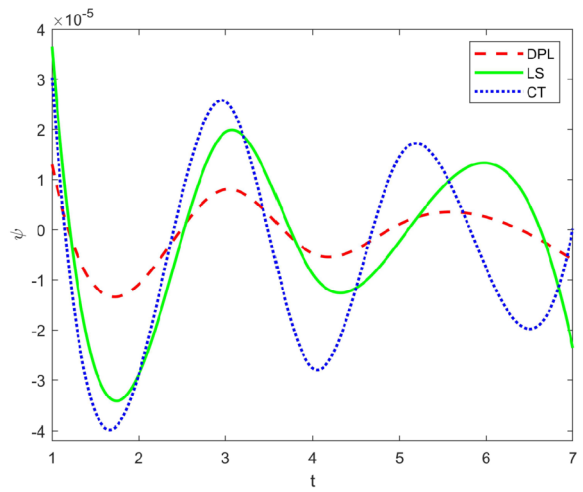


Fig. 5 Comparison of σ_z with respect to time (t) for different thermoelastic models

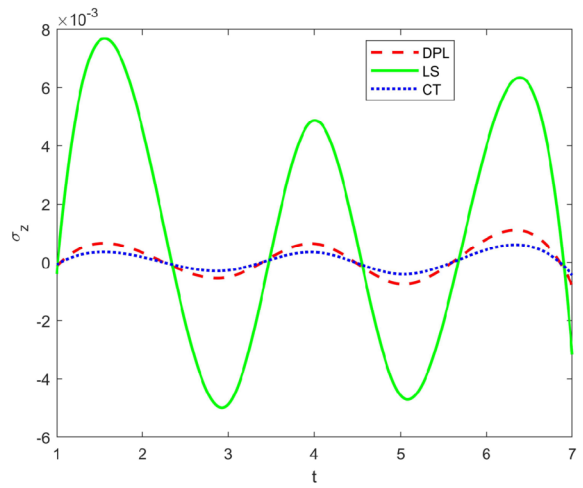
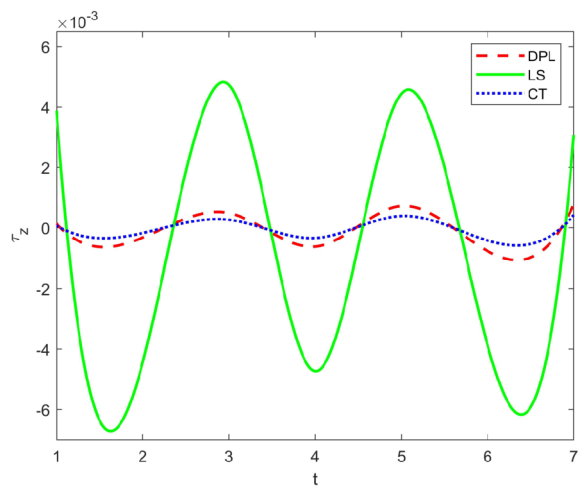


Fig. 6 Comparison of τ_z with respect to time (t) for different thermoelastic models



σ_z with the different values of t for the different thermoelastic models, namely, DPL, LS, and CT. The value of equilibrated stress component σ_z for the DPL model lies between the value of equilibrated stress component σ_z for LS and CT models. For the LS model, the equilibrated stress component σ_z has a maximum value, while for the DPL and CT models, it is nearly equal.

Figure 6 illustrates the comparison of equilibrated stress component τ_z with the different values of t . Equilibrated stress component τ_z shows wave-type behavior with the increase in t for the different thermoelastic models DPL, LS, and CT. The value of equilibrated stress component τ_z for the DPL model lies between the value of equilibrated stress component τ_z for LS and CT thermoelastic models. It is also noticed from Figs. 5 and 6 that τ_z behavior is opposite to that of τ_z .

8.2 Effect of nonlocal parameter on different physical quantities with respect to time

Figures 7-13 represent the graphs for displacement u , temperature (T), stress τ_{zz} , change in void volume fractions ϕ , ψ and equilibrated stress vectors σ_z , τ_z versus time (t) for nonlocal as well as local parameters, when x and z are fixed as 0 and 0.1.

Figure 7 depicts the variation of the horizontal displacement component u with respect to the value of t for nonlocal as well as local thermoelastic medium. The value of the horizontal displacement component u for the nonlocal thermoelastic medium is marginally greater than the value of the horizontal displacement component u for the local thermoelastic medium, and an oscillating behavior of the horizontal displacement component u is evident.

Figure 8 shows the comparison of T with respect to the values of t for the different thermoelastic models DPL, LS, and CT. T shows wave-like behavior with the increase in t . Figure 8 shows that the value of T for a nonlocal thermoelastic media and the value of T for a local thermoelastic medium nearly coincide.

Figure 9 presents the variation of normal stress component τ_{zz} with different values of t for nonlocal and local thermoelastic medium. It is noticed that normal stress component τ_{zz} shows the wave-type propagation with the increase in t and attains its maximum at $t = 1.74$ s. Both the local and nonlocal thermoelastic media have nearly the same value for the normal stress component τ_{zz} . From this figure, very minor differences between the nonlocal and local thermoelastic material may be observed.

In both the presence and absence of nonlocal parameters, Fig. 10 shows how the void volume fraction field ϕ varies with different values of t . It is seen that when t increases, the void volume fraction field ϕ exhibits wave-like propagation. The value of void volume fraction field ϕ for nonlocal thermoelastic medium is higher than the value of void volume fraction field ϕ for local thermoelastic medium.

Figure 11 depicts the variation of void volume fraction field ψ with the various values of t . It is observed from Fig. 11 that the void volume fraction field ψ shows wave-like behavior with the increase in t . The value of void volume fraction field ψ for nonlocal thermoelastic medium is higher than the value of ψ for local thermoelastic medium. It can also be observed from Figs. 10 and 11 that void volume fraction field ϕ has exactly the opposite behavior to that of void volume fraction field ψ .

The change in the equilibrated stress component σ_z with varying values of t , both in the presence and absence of nonlocal factors, is shown in Fig. 12. Figure 12 indicates that when t increases, σ_z behaves more like a wave. The value of equilibrated stress component σ_z in the presence of a nonlocal parameter is higher than in the absence of nonlocal parameter for the regions $1.082 \text{ s} < t < 2.302 \text{ s}$, $3.423 \text{ s} < t < 4.512 \text{ s}$ and $5.62 \text{ s} < t < 6.871 \text{ s}$. The

Fig. 7 Comparison of horizontal displacement component u with respect to time (t) for nonlocal and local parameters

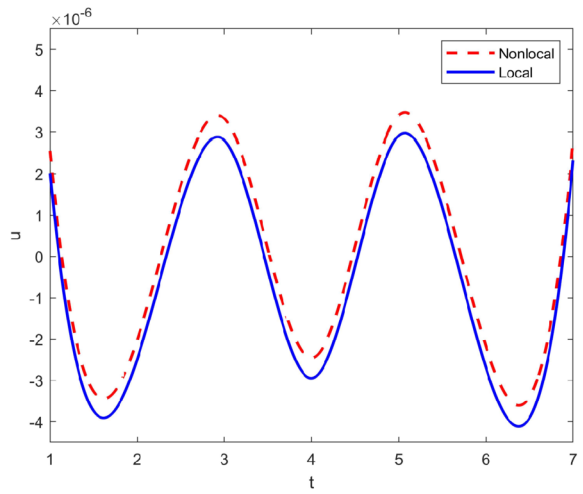


Fig. 8 Comparison of T with respect to time (t) for nonlocal and local parameters

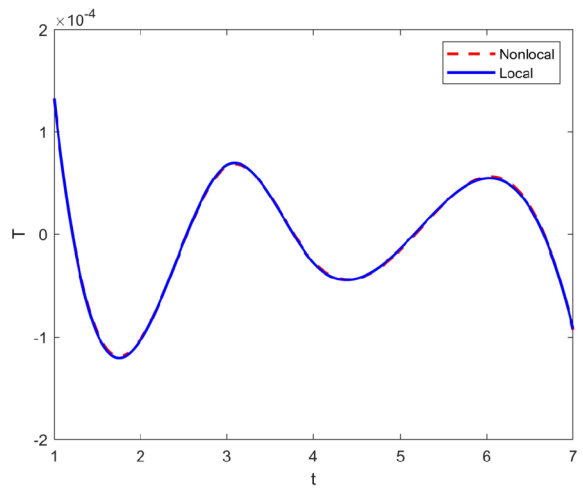


Fig. 9 Comparison of normal stress component (τ_{zz}) with respect to time (t) for nonlocal and local parameters

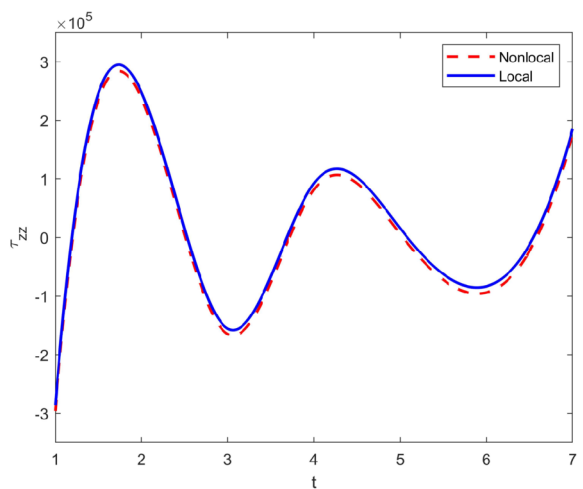


Fig. 10 Comparison of ϕ with respect to time (t) for nonlocal and local parameters

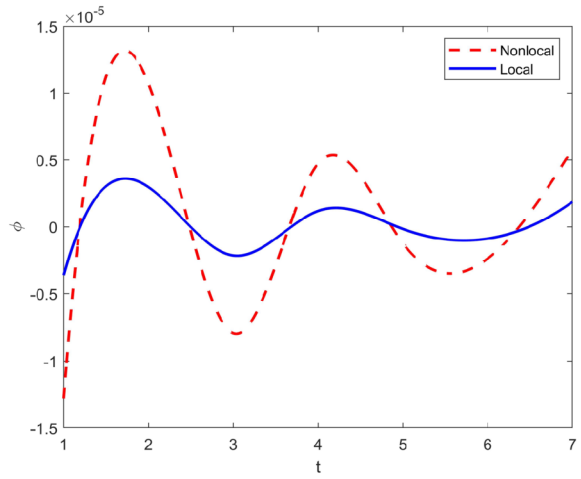


Fig. 11 Comparison of ψ with respect to time (t) for nonlocal and local parameters

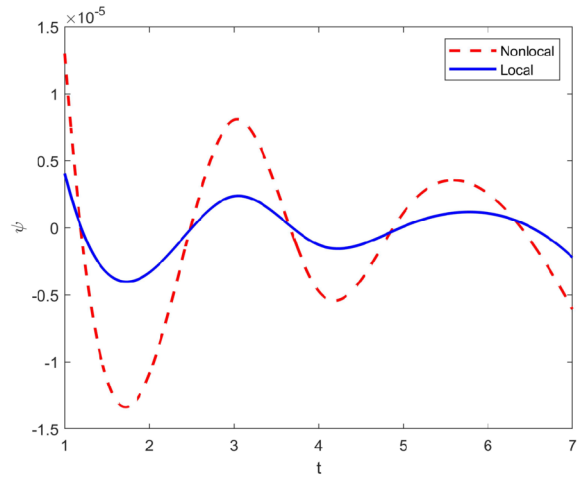


Fig. 12 Comparison of σ_z with respect to time (t) for nonlocal and local parameters

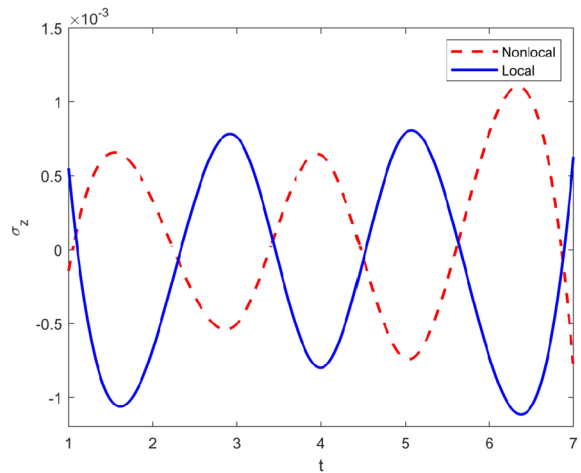
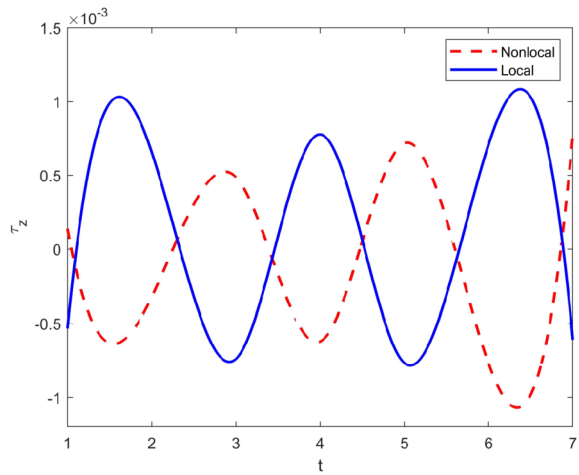


Fig. 13 Comparison of τ_z with respect to time (t) for nonlocal and local parameters



value of equilibrated stress component σ_z in the presence of nonlocal parameter is less than in the absence of nonlocal parameter for the regions $2.302 \text{ s} < t < 3.423 \text{ s}$ and $4.512 \text{ s} < t < 5.62 \text{ s}$.

Figure 13 represents the variation of equilibrated stress component τ_z with the different values of t , and τ_z shows wave-like behavior with the increase in t in the presence and absence of nonlocal parameter. For the regions $1.089 \text{ s} < t < 2.28 \text{ s}$, $3.437 \text{ s} < t < 4.502 \text{ s}$, and $5.617 \text{ s} < t < 6.875 \text{ s}$, the value of the equilibrated stress component τ_z in the presence of a nonlocal parameter is less than in the absence of a nonlocal parameter. The value of equilibrated stress component τ_z in the presence of nonlocal parameter is higher than in the absence of nonlocal parameter for the regions $2.286 \text{ s} < t < 3.437 \text{ s}$ and $4.502 \text{ s} < t < 5.67 \text{ s}$. It can also be noticed from Figs. 12 and 13 that σ_z has exactly opposite behavior to that of τ_z .

Figures 14–16 represent the graphs for displacement w , temperature above the reference temperature T , stress τ_{zz} versus time (t) for fixed values of $x = 0 \text{ m}$ and $z = 0.1 \text{ m}$ with voids and without voids, respectively.

Figure 14 represents the variation of vertical displacement component w with the different values of t in the presence and absence of void parameters. It is found from Fig. 14 that w shows wave-like behavior with the increase in t . The value of vertical displacement component w in the presence of void parameters is higher than in their absence for the regions $1.12 \text{ s} < t < 2.36 \text{ s}$, $3.49 \text{ s} < t < 4.54 \text{ s}$ and $5.65 \text{ s} < t < 6.85 \text{ s}$, respectively. For the regions of $2.36 \text{ s} < t < 3.49 \text{ s}$ and $4.54 \text{ s} < t < 5.65 \text{ s}$, respectively, the value of the vertical displacement component w in the presence of void parameters is less than in their absence. At some particular values of t , values of vertical displacement component w coincide in the presence and absence of void parameters.

The variation T with different values of t in the presence and absence of void parameters is shown in Fig. 15. Figure 15 reveals that when t increases, T exhibits wave-like behavior. The value of T in the presence of void parameters is higher than in their absence for the regions $1.12 \text{ s} < t < 2.38 \text{ s}$, $3.5 \text{ s} < t < 4.58 \text{ s}$ and $5.69 \text{ s} < t < 6.93 \text{ s}$. The value of T in the presence of void parameters is less than in their absence for the regions $2.38 \text{ s} < t < 3.5 \text{ s}$ and $4.5 \text{ s} < t < 5.59 \text{ s}$.

Figure 16 represents the variation normal stress component τ_{zz} with the different values of t in the presence and absence of void parameters. It is found from Fig. 16 that the normal

Fig. 14 Comparison of w with respect to time (t) in the presence and absence of void parameters

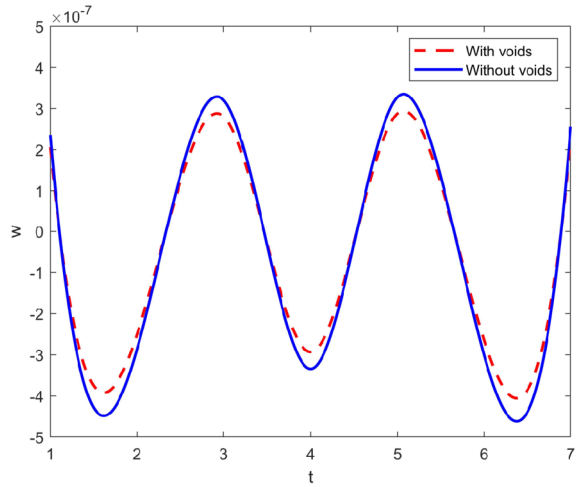


Fig. 15 Comparison of T with respect to time (t) in the presence and absence of void parameters

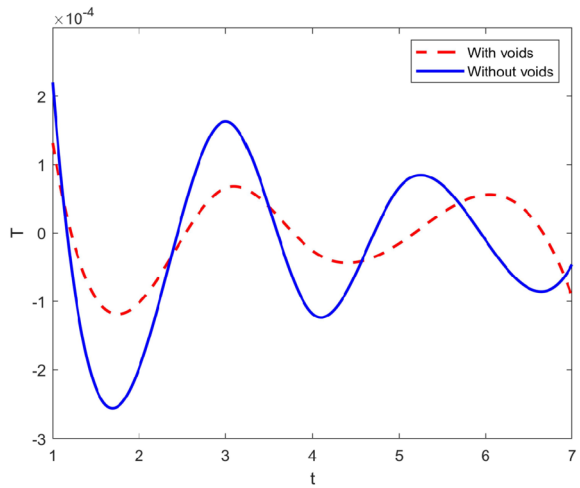
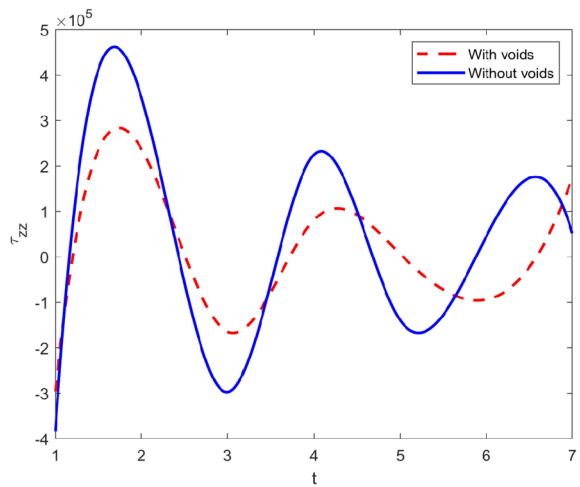


Fig. 16 Comparison of normal stress component (τ_{zz}) with respect to time (t) in the presence and absence of void parameters



stress component τ_{zz} shows wave-like behavior with the increase in t . For the regions of $1.11 \text{ s} < t < 2.28 \text{ s}$, $3.46 \text{ s} < t < 4.5 \text{ s}$, and $5.65 \text{ s} < t < 6.89 \text{ s}$, respectively, the value of the normal stress component τ_{zz} in the presence of void parameters is less than in their absence. The value of normal stress component τ_{zz} in the presence of void parameters is higher than in their absence for the regions $2.28 \text{ s} < t < 3.46 \text{ s}$ and $4.5 \text{ s} < t < 5.65 \text{ s}$. From Figs. 15 and 16, it is noticed that T and normal stress component τ_{zz} have opposite behavior.

8.3 Effect of different thermoelastic models on different physical quantities with respect to distance

Figures 17–22 represent the graphs for u , w , τ_{zz} , ϕ , ψ , σ_z and τ_z versus distance (z) when x and t are fixed at 0 and 1 for different thermoelastic models like DPL, LS, and CT.

Figure 17 depicts the comparison of w for different values of distance z . It is evident that when the distance z increases, the considered parameter w decreases smoothly for a fixed value of t . The value of w for the CT model lies between the value of w for the DPL and LS models. It is observed that the decreasing rate of w is higher for the CT model compared to the LS and DPL models.

Figure 18 shows the graph of τ_{xz} for different values of distance z . It is possible to investigate that, for DPL and CT models, the value of τ_{xz} is rapidly dropping with an increase in distance z , given a fixed value of t . For the LS model, τ_{xz} decreases smoothly as distance z increases. From Fig. 18, it is observed that the decreasing rate of τ_{xz} is higher for CT and DPL models compared to the LS model. The value of τ_{xz} is maximum for the CT model and is minimum for the LS model.

The comparison of the void volume fraction (ϕ) for various distance (z) values is displayed in Fig. 19. This graphic shows an oscillating behavior of ϕ for the CT and LS models. The maximum of ϕ is reached for the LS model. In the context of the DPL model, the value of ϕ increases for $0.1 \text{ m} < z < 0.39 \text{ m}$ and then drops for the remaining values of z .

Figure 20 depicts the comparison of void volume fraction (ψ) for different values of distance (z). An oscillatory behavior of ψ can be investigated for the LS model. ψ attains its maximum for the LS model. The value of ψ is decreasing for certain values of z and then increasing for the remaining values of z for DPL and CT models. Figures 19 and 20 show that for the three thermoelastic models, namely, DPL, LS, and CT, ϕ behaves in the opposite way as ψ .

σ_z and τ_z show wave-like behavior in Figs. 21–22, and the values of the considered parameters σ_z and τ_z for LS model are higher than for DPL and CT models. In Fig. 21, the value of σ_z decreases up to $z = 0.28 \text{ m}$, increases for $0.28 \text{ m} < z < 0.58 \text{ m}$, and then decreases again for the DPL and CT models. The value of τ_z is increasing up to $z = 0.25 \text{ m}$, decreasing for $0.25 \text{ m} < z < 0.59 \text{ m}$, and then again increasing for DPL and CT models in Fig. 22. From Figs. 21 and 22, it is noticed that σ_z shows the opposite behavior to that of τ_z for the different thermoelastic models.

Figure 23 reveals the comparison of horizontal displacement component u with respect to the different values of z in the presence and absence of nonlocal parameters. It is seen that when the distance z increases, the value of the horizontal displacement component u decreases significantly. When there are nonlocal parameters present, the value of the horizontal displacement component u is higher than when nonlocal parameters are absent. Significant impact of nonlocal parameters can be observed from this figure. The remarkable difference between the value of horizontal displacement component u in the presence of nonlocal parameters and the absence of nonlocal parameters can be revealed.

Fig. 17 Comparison of vertical displacement component w with respect to distance (z) for different thermoelastic models

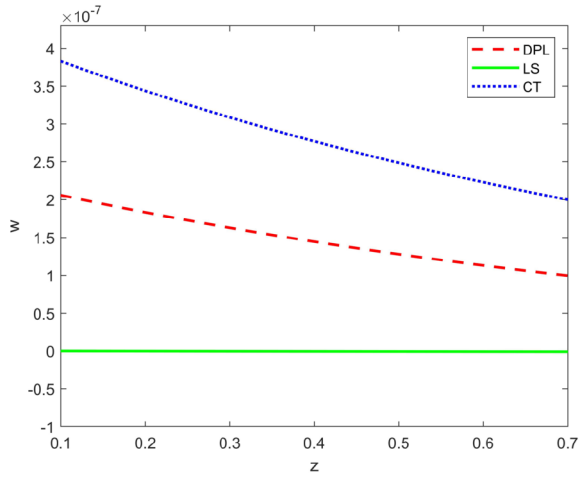


Fig. 18 Comparison of tangential stress (τ_{xz}) with respect to distance (z) for different thermoelastic models

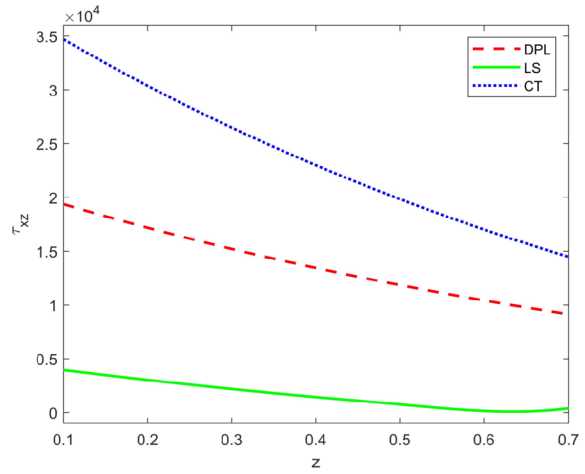


Fig. 19 Comparison of ϕ with respect to distance (z) for different thermoelastic models

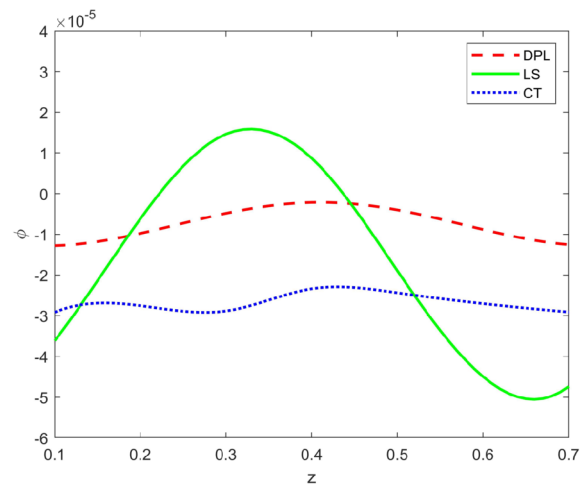


Fig. 20 Comparison of ψ with respect to distance (z) for different thermoelastic models

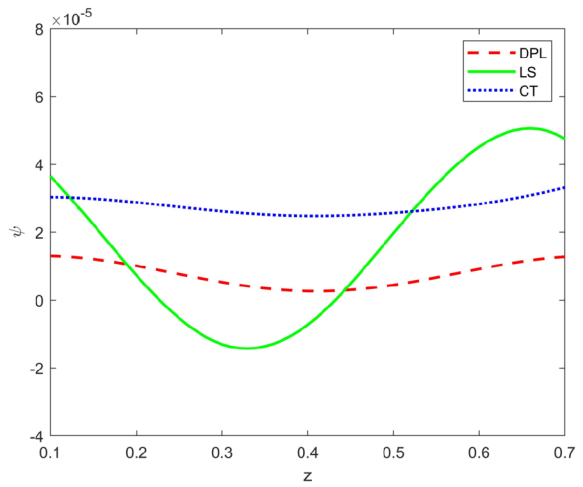


Fig. 21 Comparison of σ_z with respect to distance (z) for different thermoelastic models

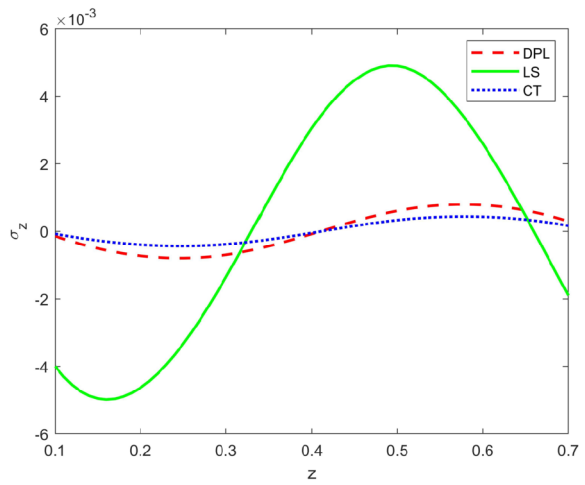


Fig. 22 Comparison of τ_z with respect to distance (z) for different thermoelastic models

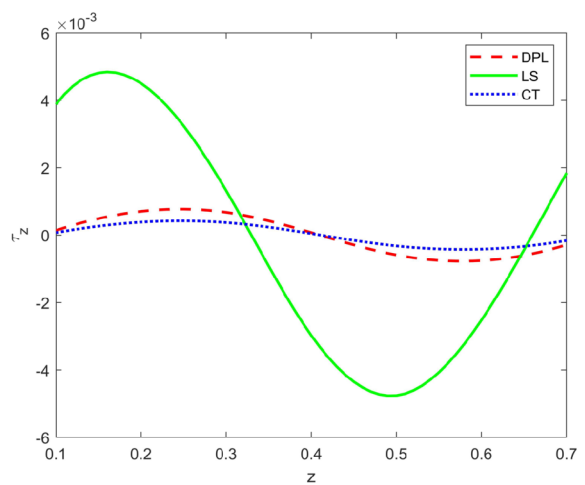
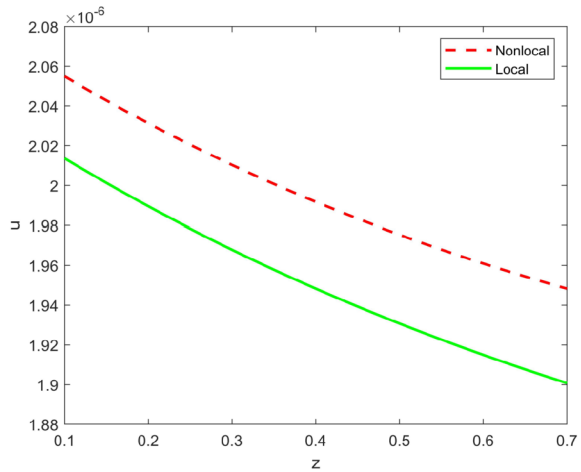


Fig. 23 Comparison of horizontal displacement component u with respect to distance (z) for nonlocal and local parameters



8.4 Effect of nonlocal and void parameters on different physical quantities with respect to distance

Figure 24 shows the variation of normal stress component τ_{zz} with respect to the different values of z in the presence and absence of nonlocal parameters. It is noted that when the distance z increases, the value of the normal stress component τ_{zz} decreases significantly. The value of normal stress component τ_{zz} in the absence of nonlocal parameters is higher than in the presence of nonlocal parameters. Initially, differences between them are small and differences are increasing with the increasing distance. The significant impact of void parameters can be observed in this figure. It is possible to observe the significant difference in the value of the normal stress component τ_{zz} in the presence void parameters and in their absence.

Figure 25 reveals the comparison of the vertical displacement component w with respect to the different values of z in the presence and absence of void parameters. It is noted that as the distance z increases, the value of the vertical displacement component w gradually decreases. The value of w in the presence of void parameters is lower than in the absence of void parameters. This figure illustrates the significant impact of void parameters. The remarkable difference between the value of the vertical displacement component w in the presence of void parameters and in their absence can be revealed.

Figure 26 reveals the comparison of tangential stress component τ_{xz} with respect to the different values of z in the presence and absence of void parameters. It is noted that as the distance z increases, the value of the tangential stress component τ_{xz} consistently decreases. When void parameters are present, the value of w is less than the tangential stress component τ_{xz} when void parameters are absent. The significant impact of void parameters can be observed in this figure. The remarkable difference between the value of tangential stress component τ_{xz} in the presence of void parameters and in their absence can be revealed.

Figures 27–32 provide 3D surface curves for the physical quantities, including $Re(T)$, normal stress component $Re(\tau_{zz})$ change in void volume fraction fields $Re(\phi)$ and $Re(\psi)$, equilibrated stress component $Re(\sigma_z)$, to study the impact of nonlocality and double voids in a nonlocal isotropic thermoelastic medium in the context of the dual-phase-lag (DPL) model. These data are crucial for understanding how these physical quantities relate to the vertical component of distance (z). All physical variables satisfy the boundary requirements.

Fig. 24 Comparison of normal stress component (τ_{zz}) with respect to distance (z) for nonlocal and local parameters

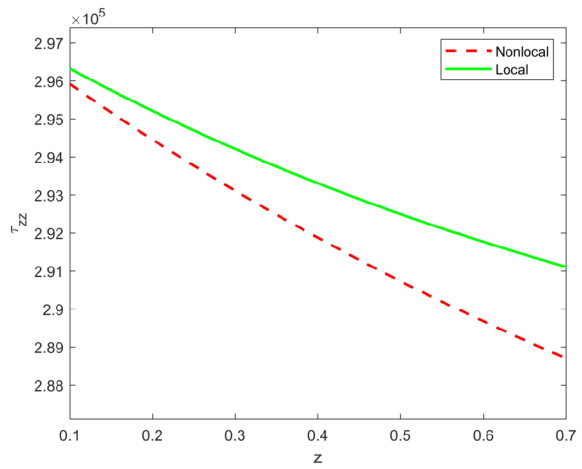


Fig. 25 Comparison of vertical displacement component w with respect to distance (z) in the presence and absence of void parameters

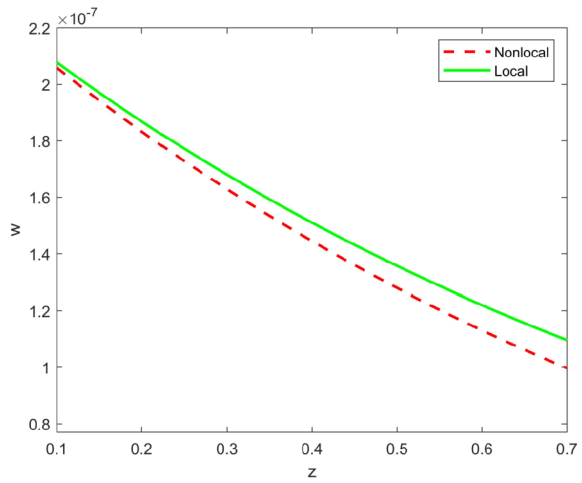


Fig. 26 Comparison of tangential stress (τ_{xz}) with respect to distance (z) in the presence and absence of void parameters

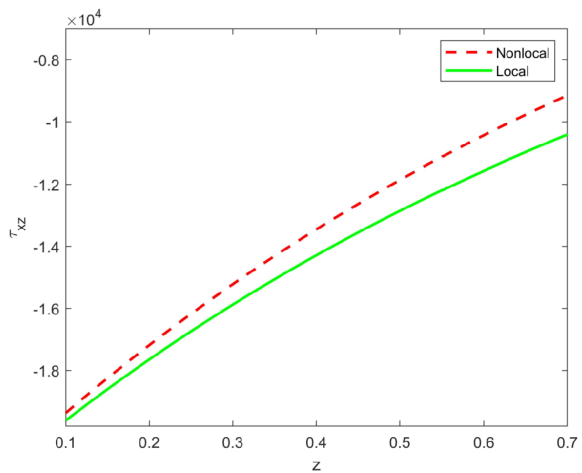


Fig. 27 Surface of $Re(T)$ for $x \in [0.1, 0.9]$ and $t \in [1, 9]$

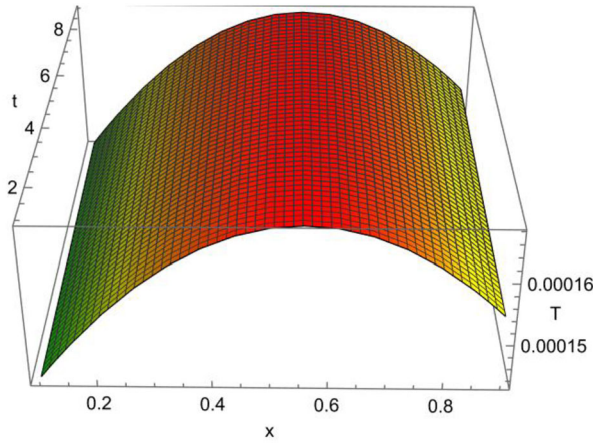


Fig. 28 Surface of $Re(\tau_{zz})$ for $x \in [0.1, 0.9]$ and $t \in [1, 9]$

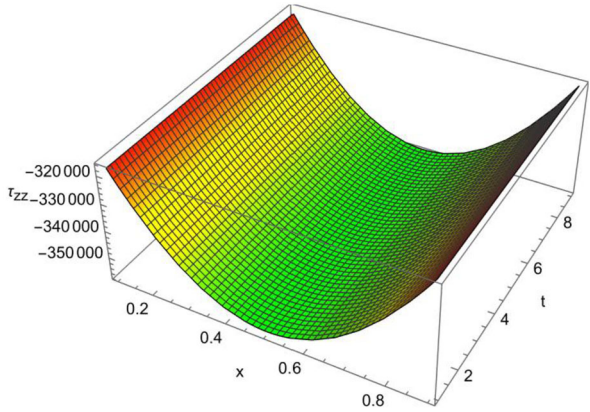


Fig. 29 Surface of $Re(\psi)$ for $x \in [0.1, 0.9]$ and $t \in [1, 9]$

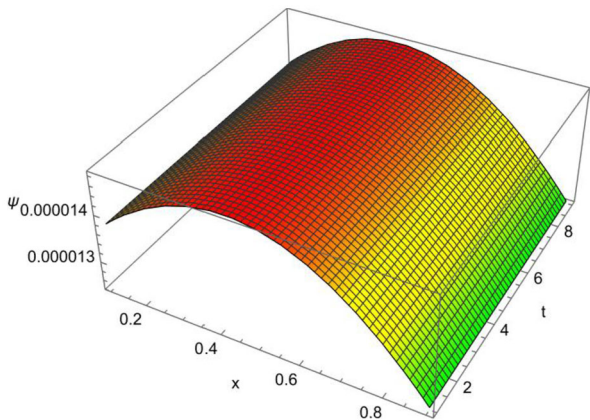


Fig. 30 Surface of $Re(T)$ for $x \in [1, 9]$ and $z \in [0.1, 0.9]$

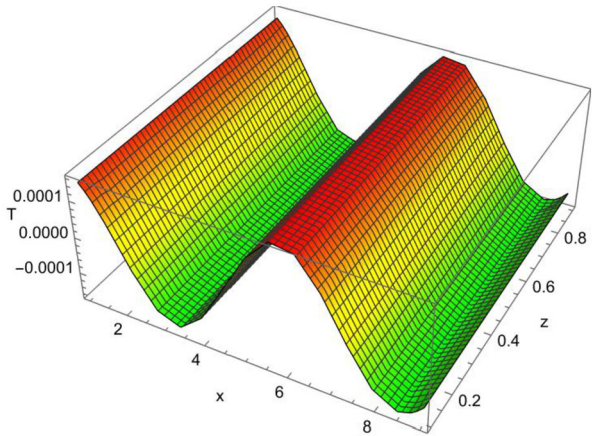


Fig. 31 Surface of $Re(\phi)$ for $x \in [1, 9]$ and $z \in [0.1, 0.9]$

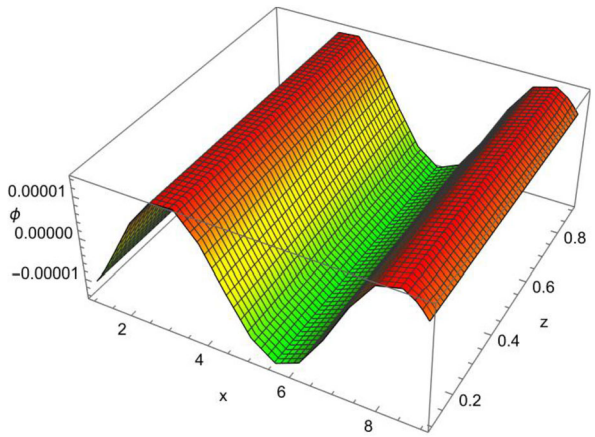
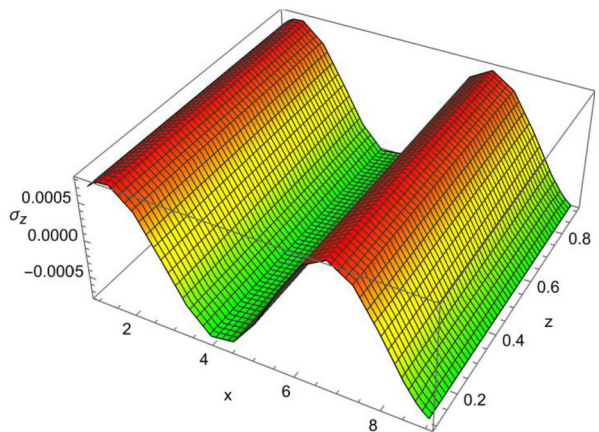


Fig. 32 Surface of $Re(\sigma_z)$ for $x \in [1, 9]$ and $z \in [0.1, 0.9]$



Assumptions and limitations of the adopted model

The values of τ_q and τ_T for a few metals have been found by Tzou (1995). The ratio τ^* (where $\tau^* = \frac{\tau_T}{\tau_q}$) is estimated by Tzou to be approximately 163 for copper, 120 for gold and silver, and 72 for lead (Ref. Chandrasekharaiah 1998). Hence, in these cases, Eq. $K \left(1 + \tau_T \frac{\partial}{\partial t}\right) \nabla^2 T = \rho C_V \left(1 + \tau_q \frac{\partial}{\partial t}\right) \frac{\partial T}{\partial t}$ is not appropriate for investigating wave-like thermal signals. For such investigations, one needs to employ a temperature equation in which both the phase-lags τ_q and τ_T are incorporated and which is hyperbolic.

9 Some applications of the present work

Voids: The porous media theory has important applications in the field of applied science and engineering. It has a wide range of applications in mechanics (acoustics, geomechanics, soil mechanics, and rock mechanics), engineering (petroleum engineering, construction engineering), geosciences (hydrogeology, petroleum geology, and geophysics), biology and biophysics, material science, and filtration. Porous materials have a significant impact on two fields of application: (a) energy conversion and (b) energy storage, where porous materials play an important role in advancing various technologies such as fuel cells, supercapacitors, and batteries, contributing to more efficient energy utilization and storage.

Nonlocality: Eringen's nonlocal theories have the following characteristics:

- (i) Nonlocal solutions eliminate singularities predicted by the classical (local) theory of elasticity.
- (ii) Maximum stress can be used to calculate the cohesive stress that holds atomic bonds together.
- (iii) Classical elasticity is obtained when the nonlocal moduli become dirac delta functions.
- (d) The cohesive stress calculated agrees with the lattice dynamical results and experimental observations.

10 Conclusion

The present work provides a detailed analysis of thermomechanical interactions in a double porous isotropic thermoelastic medium based on nonlocal elasticity theory under the purview of the dual-phase-lag model. Normal mode analysis is employed to solve the problem. Since it provides precise values for physical quantities, this method is frequently employed in many branches of mechanics. The comparison of different physical variables for various thermoelastic models and the effects of nonlocal parameters and porosity on different physical quantities are presented graphically.

Based on theoretical analysis, numerical computation, and graphical observation of the present work, the following conclusions may be inferred:

- (a) Effect of nonlocality on different physical quantities:

The graphs of u and τ_{zz} are decreasing significantly with the increase in distance for both nonlocal as well as local thermoelastic medium. In a nonlocal thermoelastic media, u has a slightly greater value compared to a local thermoelastic medium. The value τ_{zz} for nonlocal thermoelastic medium is smaller than the value of τ_{zz} for local thermoelastic medium. u , T , τ_{zz} , ϕ , ψ , σ_z and τ_z show wave-type propagation with the increase in

time for nonlocal as well as local thermoelastic medium. ϕ , ψ , σ_z , and τ_z show wave-like behavior with the increase in distance for both local and nonlocal thermoelastic medium. ϕ has the opposite behavior to that of ψ with respect to time in the presence and absence of nonlocal parameters. σ_z has the opposite behavior to that of τ_z with respect to time in both the presence and absence of nonlocal parameters.

(b) Effect of void parameters on different physical quantities:

The graphs of w and τ_{xz} in the presence and absence of void parameters are decreasing significantly with the increase in distance. In the absence of void parameters, w has a greater value than when void parameters are present. In the absence of void parameters, τ_{xz} has a greater value than in the presence of void parameters. w , T , and τ_{zz} show wave-type propagation with the increase in time in the presence of voids as well as in the absence of void parameters. T has the opposite behavior to that of τ_{zz} with respect to time in the presence and absence of void parameters.

(c) Effect of different thermoelastic models on different physical quantities:

The values of w and τ_{xz} are decreasing significantly with the increase in distance for the thermoelastic models DPL and CT compared to the LS model. The values of w and τ_{xz} are maximum for the CT model and minimum for the LS model. The values of w and τ_{xz} for the DPL model lie between the values of w and τ_{xz} for CT and LS models. u , T , τ_{xz} , ψ , σ_z and τ_z show wave-type propagation with the increase in time for different thermoelastic models like DPL, LS, and CT. In the context of the LS model, the parameters ϕ , ψ , σ_z , and τ_z exhibit wave-like behavior as distance increases. For various models, ϕ behaves in the opposite way to ψ , and σ_z behaves in the opposite way to τ_z .

Appendix A

$$N_1 = \frac{p_{30} + p_{56}}{p_{17}}, N_2 = \frac{p_{31} + p_{57} + p_{71} + s_{10} + s_{24}}{p_{17}}, N_3 = \frac{p_{32} + p_{58} + p_{72} + s_{11} + s_{25}}{p_{17}},$$

$$N_4 = \frac{p_{33} + p_{59} + p_{73} + s_{12} + s_{26}}{p_{17}}, N_5 = \frac{p_{34} + p_{74} + s_{13} + s_{27}}{p_{17}},$$

$$s_1 = a_{12}a_{17} - a_{20}, s_2 = a_{12}p_5 - p_9 - a_{16}p_{11} - a_{11}a_{20}, s_3 = a_{12}p_6 - a_{11}p_9 + a_{16}p_{12},$$

$$s_4 = a_{15}a_{17} - a_{19}, s_5 = a_{15}p_5 - p_{35} - a_{11}a_{19} - a_{16}p_{43}, s_6 = a_{15}p_6 - a_{11}p_{35} + a_{16}p_{37},$$

$$s_7 = a_{15}a_{20} - a_{12}a_{19}, s_8 = a_{12}a_{17}a_{24} - a_{15}a_{23} + p_{60}, s_9 = a_{15}p_{12} - a_{12}p_{37} + a_{11}p_{60},$$

$$s_{10} = a_4s_4 - a_4a_7s_1, s_{11} = a_4s_5 + a_4a_6s_4 - a_4a_7s_2 - a_4a_8s_7 + a_4a_{10}s_8,$$

$$s_{12} = a_4s_6 + a_4a_6s_5 - a_4a_7s_3 - a_4a_8p_{68} + a_4a_{10}s_{10}, s_{13} = a_4a_6s_6, s_{14} = -a_{23} - a_{13}p_{11},$$

$$s_{15} = a_{12}p_7 + p_{10} - a_{11}a_{23} + a_{13}p_{12} - a_{14}p_{11}, s_{16} = a_{12}p_8 + a_{11}p_{10} + a_{14}p_{12},$$

$$s_{17} = a_{13}p_{42} + a_{24}, s_{18} = a_{15}p_7 - p_{36} + a_{11}a_{24} + a_{13}p_{37} + a_{14}p_{42},$$

$$s_{19} = a_{15}p_8 - a_{11}p_{36} + a_{14}p_{37}, s_{20} = a_{12}a_{24} - a_{15}a_{23} + a_{13}p_{60},$$

$$s_{21} = a_{15}p_{10} - a_{12}p_{36} + a_{14}p_{60}, s_{22} = p_{60} - a_{15}p_{11} - a_{12}p_{42},$$

$$s_{23} = a_{15}p_{12} - a_{12}p_{37} + a_{11}p_{60}, s_{24} = a_5a_7s_{14} - a_5s_{17},$$

$$s_{25} = a_5a_7s_{15} - a_5s_{18} - a_6s_{17} + a_5a_8s_{20} - a_5a_9s_{22},$$

$$s_{26} = a_5a_7s_{16} - a_5s_{19} - a_5a_6s_{18} + a_5a_8s_{21} - a_5a_9s_{23}, s_{27} = -a_5a_6s_{19},$$

$$\begin{aligned}
 p_1 &= a_1 + a_6, p_2 = a_1 a_6, p_3 = a_{21} + a_{25}, p_4 = a_{21} a_{25} - a_{22} a_{27}, p_5 = a_{17} a_{25} + a_{18}, \\
 p_6 &= a_{18} a_{25} - a_{22} a_{26}, p_7 = a_{17} a_{27} - a_{26}, p_8 = a_{18} a_{27} - a_{26} a_{21}, p_9 = a_{20} a_{25} - a_{22} a_{23}, \\
 p_{10} &= a_{20} a_{27} - a_{21} a_{23}, p_{11} = a_{23} a_{17}, p_{12} = a_{20} a_{26} - a_{23} a_{18}, p_{13} = a_1 a_8, p_{14} = a_1 a_9, \\
 p_{15} &= a_1 a_{10}, p_{16} = -a_{23} a_{17}, p_{17} = 1 - a_{13} a_{17}, p_{18} = p_3 + a_{11} - p_5 a_{13} - a_{14} a_{17}, \\
 p_{19} &= p_4 + p_3 a_{11} - p_6 a_{13} - p_5 a_{14} + p_7 a_{16}, p_{20} = a_{11} p_4 - a_{14} p_6 + a_{16} p_8, \\
 p_{21} &= a_{12} - a_{20} p_{13}, p_{22} = a_{12} p_3 - p_9 p_{13} - a_{14} a_{20} - a_{16} a_{23}, p_{23} = a_{12} p_4 - a_{14} p_9 + a_{16} p_{10}, \\
 p_{24} &= a_{12} a_{17} - a_{20}, p_{25} = a_{12} p_5 - a_{11} a_{20} + a_{16} p_{16} - p_9, p_{26} = a_{12} p_6 - a_{11} p_9 + a_{16} p_{12}, \\
 p_{27} &= a_{23} + a_{13} p_{16}, p_{28} = a_{12} p_7 - p_{10} + a_{11} a_{23} + a_{13} p_{12} + a_{14} p_{16}, \\
 p_{29} &= a_{12} p_8 - a_{11} p_{10} + a_{14} p_{12}, p_{30} = p_{18} + p_1 p_{17} - a_8 p_{21} + a_9 p_{24} - a_{10} p_{27}, \\
 p_{31} &= p_2 p_{17} + p_{19} + p_1 p_{18} - a_8 p_{22} - p_{13} p_{21} + a_9 p_{25} + p_{14} p_{24} - a_{10} p_{28} - p_{15} p_{27}, \\
 p_{32} &= p_{20} + p_1 p_{19} + p_2 p_{18} - a_8 p_{23} - p_{13} p_{22} + a_9 p_{26} + p_{14} p_{25} - a_{10} p_{29} - p_{15} p_{28}, \\
 p_{33} &= p_1 p_{20} + p_2 p_{19} - p_{13} p_{23} + p_{14} p_{26} - p_{15} p_{29}, p_{34} = p_2 p_{20}, p_{35} = a_{19} a_{25} - a_{22} a_{24}, \\
 p_{36} &= a_{19} a_{27} - a_{21} a_{24}, p_{37} = a_{19} a_{26} - a_{18} a_{24}, p_{38} = -a_2 a_7, p_{39} = a_2 a_8, p_{40} = -a_2 a_9, \\
 p_{41} &= a_2 a_{10}, p_{42} = -a_{17} a_{24}, p_{43} = a_{17} a_{24}, p_{44} = 1 - a_{13} a_{17}, \\
 p_{45} &= a_{11} + p_3 - a_{13} p_5 - a_{14} a_{17}, p_{46} = a_{11} p_3 - a_{13} p_6 - a_{14} p_5 + a_{16} p_7, \\
 p_{47} &= a_{11} p_4 - a_{14} p_6 + a_{16} p_8, p_{48} = a_{15} - a_{13} a_{19}, \\
 p_{49} &= a_{15} p_3 - a_{13} p_{35} - a_{14} a_{19} - a_{16} a_{24}, p_{50} = a_{15} p_4 - a_{14} p_{35} + a_{16} p_{36}, \\
 p_{51} &= a_{15} a_{17} - a_{19}, p_{52} = a_{15} p_5 - p_{35} - a_{11} a_{19} + a_{16} p_{42}, p_{53} = a_{15} p_6 - a_{11} p_{35} + a_{16} p_{37}, \\
 p_{54} &= a_{15} p_7 - p_{36} + a_{11} a_{24} + a_{13} p_{37} - a_{14} p_{43}, p_{55} = a_{15} p_8 - a_{11} p_{36} + a_{14} p_{37}, \\
 p_{56} &= p_{38} p_{44}, p_{57} = p_{38} p_{45} + p_{39} p_{48} + p_{40} p_{51} - a_{13} p_{41} p_{43} + a_{24} p_{41}, \\
 p_{58} &= p_{38} p_{46} + p_{39} p_{49} + p_{40} p_{52} + p_{41} p_{54}, p_{59} = p_{38} p_{47} + p_{39} p_{50} + p_{40} p_{53} + p_{41} p_{55}, \\
 p_{60} &= a_{19} a_{23} - a_{20} a_{24}, p_{61} = a_{12} - a_{13} a_{20}, p_{62} = a_{12} p_3 - a_{13} p_9 - a_{14} a_{20} - a_{16} a_{23}, \\
 p_{63} &= a_{12} p_4 - a_{14} p_9 + a_{16} p_9, p_{64} = a_{15} - a_{13} a_{19}, p_{65} = a_{15} p_3 - a_{13} p_{35} - a_{14} a_{19} - a_{16} a_{24}, \\
 p_{66} &= a_{15} p_4 - a_{14} p_{35} + a_{16} p_{36}, p_{67} = a_{15} a_{20} - a_{12} a_{19}, p_{68} = a_{15} p_9 - a_{12} p_{35} + a_{16} p_{60}, \\
 p_{69} &= a_{12} a_{24} + a_{13} p_{60} - a_{15} a_{23}, p_{70} = a_{15} p_{10} - a_{12} p_{36} + a_{14} p_{60}, p_{71} = a_3 a_7 p_{61} - a_3 p_{64}, \\
 p_{72} &= a_3 a_7 p_{62} - a_3 p_{65} - a_3 a_6 p_{64} + a_3 a_9 p_{67} - a_3 a_{10} p_{69}, \\
 p_{73} &= a_3 a_7 p_{63} - a_3 p_{66} - a_3 a_6 p_{65} + a_3 a_9 p_{68} - a_3 a_{10} p_{70}, p_{74} = -a_3 a_6 p_{66}.
 \end{aligned}$$

Appendix B

$$\Delta = \begin{vmatrix} e_1 & e_2 & e_3 & e_4 & e_5 \\ g_1 & g_2 & g_3 & g_4 & g_5 \\ f_1 & f_2 & f_3 & f_4 & f_5 \\ l_1 & l_2 & l_3 & l_4 & l_5 \\ m_1 & m_2 & m_3 & m_4 & m_5 \end{vmatrix}, \Delta_1 = \begin{vmatrix} G & e_2 & e_3 & e_4 & e_5 \\ 0 & g_2 & g_3 & g_4 & g_5 \\ 0 & f_2 & f_3 & f_4 & f_5 \\ 0 & l_2 & l_3 & l_4 & l_5 \\ 0 & m_2 & m_3 & m_4 & m_5 \end{vmatrix},$$

$$\Delta_2 = \begin{vmatrix} e_1 & G & e_3 & e_4 & e_5 \\ g_1 & 0 & g_3 & g_4 & g_5 \\ f_1 & 0 & f_3 & f_4 & f_5 \\ l_1 & 0 & l_3 & l_4 & l_5 \\ m_1 & 0 & m_3 & m_4 & m_5 \end{vmatrix}, \Delta_3 = \begin{vmatrix} e_1 & e_2 & G & e_4 & e_5 \\ g_1 & g_2 & 0 & g_4 & g_5 \\ f_1 & f_2 & 0 & f_4 & f_5 \\ l_1 & l_2 & 0 & l_4 & l_5 \\ m_1 & m_2 & 0 & m_4 & m_5 \end{vmatrix},$$

$$\Delta_4 = \begin{vmatrix} e_1 & e_2 & e_3 & G & e_5 \\ g_1 & g_2 & g_3 & 0 & g_5 \\ f_1 & f_2 & f_3 & 0 & f_5 \\ l_1 & l_2 & l_3 & 0 & l_5 \\ m_1 & m_2 & m_3 & 0 & m_5 \end{vmatrix}, \Delta_5 = \begin{vmatrix} e_1 & e_2 & e_3 & e_4 & G \\ g_1 & g_2 & g_3 & g_4 & 0 \\ f_1 & f_2 & f_3 & f_4 & 0 \\ l_1 & l_2 & l_3 & l_4 & 0 \\ m_1 & m_2 & m_3 & m_4 & 0 \end{vmatrix}.$$

Acknowledgements We thank the reviewers for their time spent on reviewing our manuscript, careful reading and insightful comments and suggestions that lead to improve the quality of this manuscript.

Author contributions First and second authors wrote the main manuscript text and first author prepared figures. All authors reviewed the manuscript.

Funding Chandra Sekhar Mahato is thankful to the University Grants Commission, New Delhi, India for providing the NET-JRF Fellowship.

Data Availability No datasets were generated or analysed during the current study.

Declarations

Competing interests The authors declare no competing interests.

References

- Abdou, M.A., Othman, M.I.A., Tantawi, R.S., Mansour, N.T.: Effect of magnetic field on generalized thermoelastic medium with double porosity structure under L–S theory. *Indian J. Phys.* **94**, 1993–2004 (2020a). <https://doi.org/10.1007/s12648-019-01648-8>
- Abdou, M.A., Othman, M.I.A., Tantawi, R.S., Mansour, N.T.: Exact solutions of generalized thermoelastic medium with double porosity under L–S theory. *Indian J. Phys.* **94**, 725–736 (2020b). <https://doi.org/10.1007/s12648-019-01505-8>
- Biswas, S.: Thermal shock problem in porous orthotropic medium with three-phase-lag model. *Indian J. Phys.* **95**, 289–298 (2021). <https://doi.org/10.1007/s12648-020-01703-9>
- Biswas, S., Mahato, C.S.: Eigenvalue approach to study Rayleigh waves in nonlocal orthotropic layer lying over nonlocal orthotropic half-space with dual-phase-lag model. *J. Therm. Stresses* **45**, 937–959 (2022). <https://doi.org/10.1080/01495739.2022.2075503>
- Biswas, S., Mukhopadhyay, B.: Eigenfunction expansion method to analyze thermal shock behaviour in magneto-thermoelastic orthotropic medium under three theories. *J. Therm. Stresses* **41**, 366–382 (2017). <https://doi.org/10.1080/01495739.2017.1393780>
- Chandrasekharaiah, D.S.: Hyperbolic thermoelasticity: a review of recent literature. *Appl. Mech. Rev.* **51**, 705–729 (1998). <https://doi.org/10.1115/1.3098984>
- Cheng, T., Li, W., Shi, Y., et al.: Effects of mechanical boundary conditions on thermal shock resistance of ultra-high temperature ceramics. *Appl. Math. Mech.* **36**, 201–210 (2015). <https://doi.org/10.1007/s10483-015-1909-7>
- Cowin, S.C., Nunziato, J.W.: Linear elastic materials with voids. *J. Elast.* **13**, 125–147 (1983). <https://doi.org/10.1007/BF00041230>
- Eringen, A.C.: Theory of nonlocal thermoelasticity. *Int. J. Eng. Sci.* **12**, 1063–1077 (1974). [https://doi.org/10.1016/0020-7225\(74\)90033-0](https://doi.org/10.1016/0020-7225(74)90033-0)
- Eringen, A.C.: Edge dislocation on nonlocal elasticity. *Int. J. Eng. Sci.* **15**, 177–183 (1977). [https://doi.org/10.1016/0020-7225\(77\)90003-9](https://doi.org/10.1016/0020-7225(77)90003-9)
- Eringen, A.C.: A mixture theory of electromagnetism and superconductivity. *Int. J. Eng. Sci.* **36**, 525–543 (1998). [https://doi.org/10.1016/S0020-7225\(97\)00091-8](https://doi.org/10.1016/S0020-7225(97)00091-8)

- Eringen, A.C., Edelen, D.G.B.: On nonlocal elasticity. *Int. J. Eng. Sci.* **10**, 233 (1972). [https://doi.org/10.1016/0020-7225\(72\)90039-0](https://doi.org/10.1016/0020-7225(72)90039-0)
- Green, A.E., Lindsay, K.A.: Thermoelasticity. *J. Elast.* **2**, 1–7 (1972). <https://doi.org/10.1007/BF00045689>
- Green, A.E., Naghdi, P.M.: On undamped heat waves in an elastic solid. *J. Therm. Stresses* **15**, 252–264 (1992). <https://doi.org/10.1080/01495739208946136>
- Green, A.E., Naghdi, P.M.: Thermoelasticity without energy dissipation. *J. Elast.* **31**, 189–208 (1993). <https://doi.org/10.1007/BF00044969>
- Gupta, M., Mukhopadhyay, S.: A study on generalized thermoelasticity theory based on nonlocal heat conduction model with dual-phase-lag model. *J. Therm. Stresses* **42**, 1123–1135 (2019). <https://doi.org/10.1080/01495739.2019.1614503>
- Hong-Gang, W.: On the free energy and variational theorem of elastic problem in thermal shock. *Appl. Math. Mech.* **3**, 675–681 (1982). <https://doi.org/10.1007/BF01875732>
- Iesan, D.: A theory of thermoelastic materials with voids. *Acta Mech.* **60**, 67–89 (1986). <https://doi.org/10.1007/BF01302942>
- Iesan, D., Quintanilla, R.: On a theory of thermoelastic materials with a double porosity structure. *J. Therm. Stresses* **37**, 1017–1036 (2014). <https://doi.org/10.1080/01495739.2014.914776>
- Kalkal, K.K., Kadian, A., Kumar, S.: Three-phase-lag functionally graded thermoelastic model having double porosity and gravitational effect. *J. Ocean Eng. Sci.* (2021). <https://doi.org/10.1016/j.joes.2021.11.005>
- Kaur, I., Singh, K.: Functionally graded nonlocal thermoelastic nanobeam with memory-dependent derivatives. *SN Appl. Sci.* **4**, 329 (2022a). <https://doi.org/10.1007/s42452-022-05212-8>
- Kaur, I., Singh, K.: Nonlocal memory dependent derivative analysis of a photo-thermoelastic semiconductor resonator. *Mech. Solids* **48**, 529–553 (2023b). <https://doi.org/10.3103/S0025654422601094>
- Kaur, I., Lata, P., Singh, K.: Study of transversely isotropic nonlocal thermoelastic thin nano-beam resonators with multi-dual-phase-lag theory. *Arch. Appl. Mech.* **91**, 317–341 (2021a). <https://doi.org/10.1007/s00419-020-01771-7>
- Kaur, I., Singh, K., Craciun, E.M.: Recent advances in the theory of thermoelasticity and the modified models for the nanobeams: a review. *Mech. Eng.* **2**, 2 (2023b). <https://doi.org/10.1007/s44245-023-00009-4>
- Khalili, N.: Coupling effects in double porosity media with deformable matrix. *Geophys. Res. Lett.* **30**, 2163 (2003). <https://doi.org/10.1029/2003GL018544>
- Khalili, N., Selvaduri, A.P.S.: A fully coupled constitutive model for thermo-hydro-mechanical analysis in elastic media with double porosity. *Geophys. Res. Lett.* **30**, 2268–2271 (2003). <https://doi.org/10.1029/2003GL018838>
- Khurana, A., Tomar, S.K.: Wave propagation in nonlocal microstretch solid. *Appl. Math. Model.* **40**, 5858–5875 (2016). <https://doi.org/10.1016/j.apm.2016.01.035>
- Kumar, R., Vohra, R., Abo-Dahab, S.M.: Rayleigh waves in thermoelastic medium with double porosity. *MOJ Civil Eng.* **4**, 143–148 (2018). <https://doi.org/10.15406/mojce.2018.04.00112>
- Kumar, D., Singh, D., Tomar, S.K., Hirose, S., Saitoh, T., Furukawa, A.: Waves in nonlocal elastic material with double porosity. *Arch. Appl. Mech.* **91**, 4797–4815 (2021). <https://doi.org/10.1007/s00419-021-02035-8>
- Lord, H.W., Shulman, Y.: A generalized dynamical theory of thermoelasticity. *J. Mech. Phys. Solids* **15**, 299–309 (1967). [https://doi.org/10.1016/0022-5096\(67\)90024-5](https://doi.org/10.1016/0022-5096(67)90024-5)
- Mahato, C.S., Biswas, B.: State space approach to study thermal shock problem in nonlocal thermoelastic medium with double porosity. *J. Therm. Stresses* **46**(5), 415–443 (2023). <https://doi.org/10.1080/01495739.2023.2173689>
- Mondal, S., Sarkar, N., Sarkar, N.: In dual-phase-lag thermoelastic materials with voids based on Eringen's nonlocal elasticity. *J. Therm. Stresses* **42**, 1035–1050 (2019). <https://doi.org/10.1080/01495739.2019.1591249>
- Nunziato, J.W., Cowin, S.C.: A nonlinear theory of elastic materials with voids. *Arch. Ration. Mech. Anal.* **72**, 175–201 (1979). <https://doi.org/10.1007/BF00249363>
- Othman, M.I.A., Mansour, N.T.: Effect of relaxation time on generalized double porosity thermoelastic medium with diffusion. *Geomech. Eng.* **32**, 475–482 (2023). <https://doi.org/10.12989/gae.2023.32.5.475>
- Othman, M.I.A., Said, S.M., Eldemerdash, M.G.: The effect of nonlocal on poro-thermoelastic solid with dependent properties on reference temperature via the three-phase-lag model. *J. Mater. Appl.* (2023). <https://doi.org/10.32732/jma.2023.12.1.21>
- Puri, P., Cowin, S.C.: Plane waves in linear elastic materials with voids. *J. Elast.* **15**, 167–183 (1985). <https://doi.org/10.1007/BF00041991>
- Roy Choudhuri, S.K.: On a thermoelastic three-phase-lag model. *J. Therm. Stresses* **30**, 231–238 (2007). <https://doi.org/10.1080/01495730601130919>
- Said, S.M., Abd-Elaziz, E.M., Othman, M.I.A.: The effect of initial stress and rotation on a nonlocal fiber-reinforced thermoelastic medium with a fractional derivative heat transfer. *Z. Angew. Math. Mech.* (2021). <https://doi.org/10.1002/zamm.202100110>

- Said, S.M., Abd-Elaziz, E.M., Othman, M.I.A.: Effect of gravity and initial stress on a nonlocal thermo-viscoelastic medium with two-temperature and fractional derivative heat transfer. *Z. Angew. Math. Mech.* (2022a). <https://doi.org/10.1002/zamm.202100316>
- Said, S.M., Othman, M.I.A., Eldemerdash, M.G.: A novel model on nonlocal thermoelastic rotating porous medium with memory-dependent derivative. *Multidiscip. Model. Mater. Struct.* (2022b). <https://doi.org/10.1108/MMMS-05-2022-0085>
- Sarkar, N., Mondal, S., Othman, M.I.A.: L–S theory for the propagation of the photo-thermal waves in a semi-conducting nonlocal elastic medium. *Waves Random Complex Media* **32**, 2622–2635 (2022). <https://doi.org/10.1080/17455030.2020.1859161>
- Sherief, H., Saleh, H.: A half-space problem in the theory of generalized thermoelastic diffusion. *Int. J. Solids Struct.* **42**, 4484–4493 (2005). <https://doi.org/10.1016/j.ijsolstr.2005.01.001>
- Singh, D., Kumar, D., Tomar, S.K.: Plane harmonic waves in thermoelastic solid with double porosity. *Math. Mech. Solids* **25**, 869–886 (2020). <https://doi.org/10.1177/1081286519890053>
- Tomar, S., Sarkar, N.: Plane waves in nonlocal thermoelastic solid with voids. *J. Therm. Stresses* **42**, 580–606 (2019). <https://doi.org/10.1080/01495739.2018.155439>
- Tzou, D.Y.: A unique field approach for heat conduction from macro to micro scales. *J. Heat Transf.* **17**, 8–16 (1995). <https://doi.org/10.1115/1.2822329>

Publisher's Note Springer Nature remains neutral with regard to jurisdictional claims in published maps and institutional affiliations.

Springer Nature or its licensor (e.g. a society or other partner) holds exclusive rights to this article under a publishing agreement with the author(s) or other rightsholder(s); author self-archiving of the accepted manuscript version of this article is solely governed by the terms of such publishing agreement and applicable law.